The Plant Cell, Vol. 17, 1685–1703, June 2005, www.plantcell.org

Identification and Functional Analysis of in Vivo Phosphorylation Sites of the Arabidopsis BRASSINOSTEROID-INSENSITIVE1 Receptor Kinase

Xiaofeng Wang,[a] Michael B. Goshe,[b] Erik J. Soderblom,[b] Brett S. Phinney,[c] Jason A. Kuchar,[c] Jia Li,[d] Tadao Asami,[e] Shigeo Yoshida,[e] Steven C. Huber,[f] and Steven D. Clouse[a,1]

[a] Department of Horticultural Science, North Carolina State University, Raleigh, North Carolina 27695-7609
[b] Department of Molecular and Structural Biochemistry, North Carolina State University, Raleigh, North Carolina 27695-7622
[c] Proteomics Facility, Michigan State University, East Lansing, Michigan 48824
[d] Department of Botany and Microbiology, University of Oklahoma, Norman, Oklahoma 73019-0245
[e] RIKEN, Institute of Physical and Chemical Research, Wako, Saitama, 351-0198 Japan
[f] U.S. Department of Agriculture, Agricultural Research Service, University of Illinois, Urbana, Illinois 61801-3838

Brassinosteroids (BRs) regulate multiple aspects of plant growth and development and require an active BRASSINOSTEROID-INSENSITIVE1 (BRI1) and BRI1-ASSOCIATED RECEPTOR KINASE1 (BAK1) for hormone perception and signal transduction. Many animal receptor kinases exhibit ligand-dependent oligomerization followed by autophosphorylation and activation of the intracellular kinase domain. To determine if early events in BR signaling share this mechanism, we used coimmunoprecipitation of epitope-tagged proteins to show that in vivo association of BRI1 and BAK1 was affected by endogenous and exogenous BR levels and that phosphorylation of both BRI1 and BAK1 on Thr residues was BR dependent. Immunoprecipitation of epitope-tagged BRI1 from *Arabidopsis thaliana* followed by liquid chromatography–tandem mass spectrometry (LC/MS/MS) identified S-838, S-858, T-872, and T-880 in the juxtamembrane region, T-982 in the kinase domain, and S-1168 in C-terminal region as in vivo phosphorylation sites of BRI1. MS analysis also strongly suggested that an additional two residues in the juxtamembrane region and three sites in the activation loop of kinase subdomain VII/VIII were phosphorylated in vivo. We also identified four specific BAK1 autophosphorylation sites in vitro using LC/MS/MS. Site-directed mutagenesis of identified and predicted BRI1 phosphorylation sites revealed that the highly conserved activation loop residue T-1049 and either S-1044 or T-1045 were essential for kinase function in vitro and normal BRI1 signaling in planta. Mutations in the juxtamembrane or C-terminal regions had only small observable effects on autophosphorylation and in planta signaling but dramatically affected phosphorylation of a peptide substrate in vitro. These findings are consistent with many aspects of the animal receptor kinase model in which ligand-dependent autophosphorylation of the activation loop generates a functional kinase, whereas phosphorylation of noncatalytic intracellular domains is required for recognition and/or phosphorylation of downstream substrates.

INTRODUCTION

Brassinosteroids (BRs) are endogenous plant growth–promoting hormones found throughout the plant kingdom in seeds, pollen, and young vegetative tissues. BRs act at nanomolar concentrations to regulate cellular expansion, differentiation, and proliferation, and the phenotype of mutants affected in BR biosynthesis or signaling clearly show that these plant steroids are essential for normal organ elongation, vascular differentiation, male fertility, timing of senescence, and leaf development (Clouse and Sasse, 1998; Altmann, 1999). Perception and transduction of the BR signal requires a membrane-localized Leu-rich repeat (LRR) receptor-like kinase (RLK), encoded in *Arabidopsis thaliana* by the *BRASSINOSTEROID-INSENSITIVE1* (*BRI1*) gene (Clouse, 2002; Thummel and Chory, 2002; Peng and Li, 2003; Wang and He, 2004). Mutational analyses of BRI1 in Arabidopsis and several crop species have demonstrated an indispensable role for this RLK in BR signal transduction (Clouse et al., 1996; Kauschmann et al., 1996; Li and Chory, 1997; Noguchi et al., 1999; Bishop, 2003). Moreover, biochemical studies in Arabidopsis have shown that BRI1 is an essential component of the BR receptor (Wang et al., 2001; Kinoshita et al., 2005).

The recent discovery of BRI1-ASSOCIATED RECEPTOR KINASE1 (BAK1), a second LRR RLK that interacts with BRI1 in vitro and in vivo, suggests that receptor kinase heterodimerization may also play an important role in BR signal transduction (Li et al., 2002; Nam and Li, 2002). Genetic analysis demonstrated

[1] To whom correspondence should be addressed. E-mail steve_clouse@ncsu.edu; fax 919-515-2505.
The author responsible for distribution of materials integral to the findings presented in this article in accordance with the policy described in the Instructions for Authors (www.plantcell.org) is: Steven D. Clouse (steve_clouse@ncsu.edu).
Article, publication date, and citation information can be found at www.plantcell.org/cgi/doi/10.1105/tpc.105.031393.

a role for BAK1 in BR signaling, and a direct physical interaction between BRI1 and BAK1 was found both in yeast cells and Arabidopsis plants by coimmunoprecipitation experiments with tagged proteins (Li et al., 2002; Nam and Li, 2002). Recently, fluorescence lifetime imaging microscopy (FLIM) coupled with fusions of BRI1 and BAK1 to cyan and yellow fluorescent proteins was used to show heterodimerization of BRI1 and BAK1 in protoplast endosomes (Russinova et al., 2004), confirming the validity of coimmunoprecipitation as an assay of BRI1/BAK1 association in planta.

BRI1 and BAK1 belong to a large monophyletic gene family of Arabidopsis LRR RLKs with an organization of functional domains similar to that of animal receptor kinases, including a putative extracellular ligand binding domain, a single-pass transmembrane sequence, and an intracellular kinase domain (Shiu and Bleecker, 2001; Cock et al., 2002). Besides BRI1 and BAK1, several other LRR RLK subfamily members involved in multiple aspects of Arabidopsis growth and development have been extensively characterized (reviewed in Becraft, 2002; Haffani et al., 2004; Torii, 2004). In no case, however, has a complete functional characterization of a single LRR RLK been accomplished, including detailed biochemical analysis of ligand-induced oligomerization and kinase domain autophosphorylation on specific residues in planta.

The well-established paradigm for mammalian receptor kinase action confirms that ligand-induced oligomerization followed by autophosphorylation of the cytoplasmic domain are essential elements for both receptor kinase activation and generation of reversible protein–protein interaction motifs that transduce the signal to specific downstream components of the pathway (Schlessinger, 2000, 2002). The receptor Tyr kinases (RTKs), such as insulin and epidermal growth factor receptors, and receptor Ser/Thr kinases, typified by the transforming growth factor-β (TGF-β) family of receptors, both exhibit this type of underlying regulatory mechanism (Massague, 1998; Schlessinger, 2000). Phosphorylation of the cytoplasmic domain of receptor kinases can occur on multiple sites in the catalytic kinase domain, in the juxtamembrane region lying between the transmembrane domain and the kinase domain, and in the short C-terminal region immediately following the 12 conserved subdomains of the catalytic kinase (Huse and Kuriyan, 2002). Phosphorylation of one to three residues in the kinase activation loop, a segment beginning with the highly conserved DFG in subdomain VII and terminating most often with APE in subdomain VIII, is a very common mechanism of general kinase activation and in some cases also affects binding of kinase substrates (Johnson et al., 1996; Adams, 2003). Autophosphorylation of juxtamembrane and C-terminal regions, which show much less sequence conservation among receptor kinases than the activation loop, generates docking sites for specific kinase substrates (Pawson, 2004). Moreover, phosphorylation of noncatalytic regions in the cytoplasmic domain may also lead to a general kinase catalytic domain activation by a variety of mechanisms (Pawson, 2002).

To thoroughly characterize plant RLK function, it is essential to understand the role of receptor dimerization and cytoplasmic domain autophosphorylation, including identification of specific phosphorylation sites in vivo and their functional significance. Very little is currently known about specific phosphorylation sites in plant RLKs. Using matrix-assisted laser desorption ionization mass spectrometry (MALDI/MS), we previously found that recombinant BRI1 kinase domain autophosphorylated on twelve Ser and Thr residues in vitro, including five in the juxtamembrane region, five in the kinase domain (with three sites in the activation loop), and two in the C-terminal region (Oh et al., 2000). However, the biological significance of these phosphorylation events was not addressed in that report. The identification of in vivo sites of phosphorylation in several plant RLKs using liquid chromatography–tandem mass spectrometry (LC/MS/MS) of tryptic peptides from plasma membrane proteins was recently reported (Nuhse et al., 2004). Although providing a very valuable initial database, the biological function of these phosphorylation events was not examined in this broad proteomic approach. Tryptic phosphopeptide mapping and site-directed mutagenesis of Ser and Thr residues has been used to study the phosphorylation status of several recombinant RLK kinase domains in vitro, but no analysis of specific in vivo phosphorylation sites was reported in these RLK studies (Schulze-Muth et al., 1996; Shah et al., 2001; Liu et al., 2002; Yoshida and Parniske, 2005).

To understand more clearly the mechanism of early events in BR signal transduction as well as RLK activation in general, we used LC/MS/MS analysis of immunoprecipitated BRI1-Flag protein to show that this RLK is phosphorylated on specific Ser and Thr residues in vivo. We also addressed the BR dependence of BRI1 and BAK1 association and phosphorylation in vivo and assessed the functional significance of specific Ser and Thr residues both in vitro with respect to kinase activity and in vivo by the ability of mutated versions of a BRI1-Flag transgene to rescue the dwarf phenotype of the *bri1-5* BR-insensitive mutant.

RESULTS

Brassinolide-Dependent Association of BRI1 and BAK1 in Vivo

If dimerization of BRI1/BAK1 occurs as a result of BR perception, it would suggest mechanistic similarities to both animal RTK and TGF-β receptor activities (Li et al., 2002; Nam and Li, 2002). To assess the effect of BR levels on the in vivo association of BRI1 and BAK1, we used the same double transgenic line originally employed by Li et al. (2002) to demonstrate BRI1/BAK1 interaction by coimmunoprecipitation. Transgenic plants expressing both BRI1-Flag and BAK1–green fluorescent protein (GFP) C-terminal fusions were grown in shaking liquid culture for 6 d. Half of the flasks were then treated with brassinazole (BRZ), a highly specific inhibitor of BR biosynthesis, for an additional 5 d to reduce endogenous BR levels (Asami et al., 2000). At the end of 11 d of growth, one-half of the –BRZ plants and one-half of the +BRZ plants were treated with 0.1 μM brassinolide (BL) for 90 min. Total membrane protein was purified from each sample, including three control lines, and BRI-Flag was immunoprecipitated from the solubilized membranes as described (Li et al., 2002). The immunoprecipitated protein was confirmed to be BRI1 by ion trap and quadrapole-time-of-flight (QTOF) LC/MS/MS (data not shown). Figures 1A and 1B show that by loading equal amounts of solubilized membrane proteins on SDS-PAGE gels, approximately equal levels of BRI1-Flag and BAK1-GFP

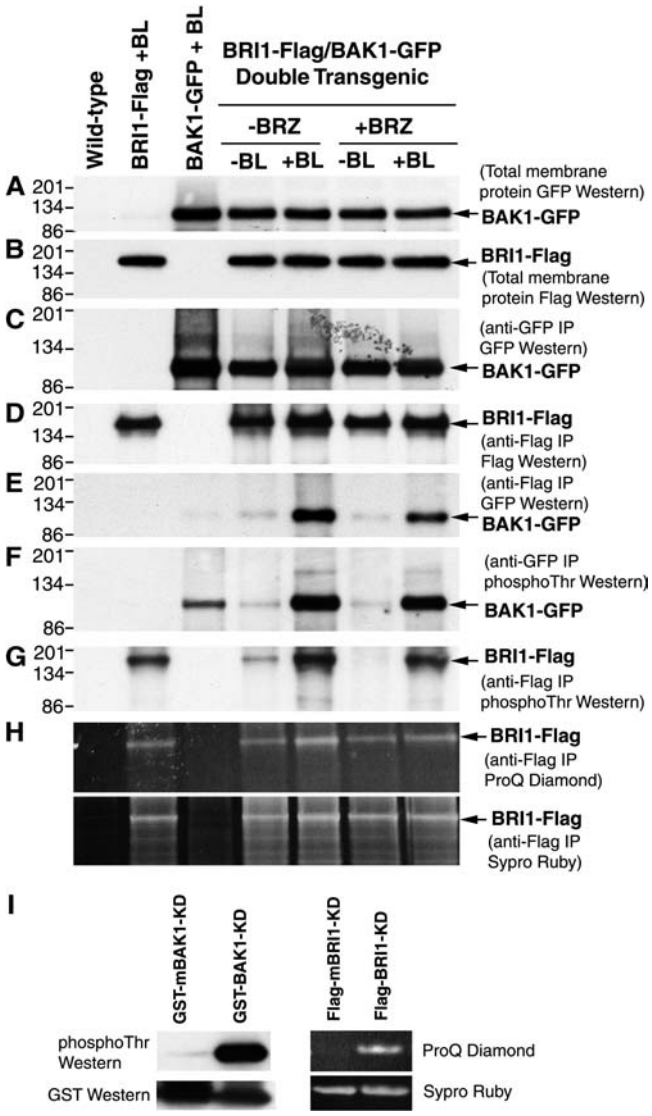

Figure 1. BL Dependence of Early Events in BR Signaling.

Transgenic Arabidopsis plants expressing both BRI1-Flag and BAK1-GFP were grown as described in the text. Total membrane protein was purified from each sample, including an untreated, untransformed (wild-type) control, and two BL-treated lines expressing BRI-Flag or BAK1-GFP alone. Immunoprecipitation of solubilized membrane proteins was performed as described (Li et al., 2002), and equal amounts of protein were separated by SDS-PAGE followed by protein gel blot analysis as indicated. The entire experiment (**[A]** to **[I]**) was repeated three times with consistent results. Numbers to the left of each blot indicate migration of molecular mass markers (kD).

(A) to **(D)** Approximately equal amounts of BRI1-Flag and BAK1-GFP were present in total membrane extracts and immunoprecipitated samples, indicating that BL or BRZ treatment did not affect the total level of these proteins in planta.

(E) Association of BRI1 and BAK1 in vivo, as determined by coimmunoprecipitation, is BL dependent.

(F) and **(G)** Phosphorylation of Thr residues in BRI1-FLAG and BAK1-GFP is BL dependent (note that the FLAG epitope tag has no Thr residues).

were detected in all treatments by protein gel blot analysis with anti-Flag or anti-GFP antibodies. Moreover, the amount of BRI1-Flag and BAK1-GFP immunoprecipitated from equal amounts of solubilized membrane protein was unaffected by BL or BRZ treatment (Figures 1C and 1D), and there was no nonspecific interaction between anti-Flag antibody and BAK1-GFP or anti-GFP antibody and BRI1-Flag. To determine the amount of BAK1-GFP brought down with BRI1-Flag under each treatment, BRI1-Flag was immunoprecipitated with anti-Flag antibody and the amount of associated BAK1-GFP was determined by immunoblot analysis with anti-GFP antibody. As indicated in Figure 1E, BAK1-GFP coimmunoprecipitated with BRI1-FLAG, as expected, and BL treatment increased the amount of BAK1-GFP associated with BRI1-Flag. Moreover, reduction of endogenous BR levels by BRZ treatment reduced the association of BAK1-GFP and BRI1-FLAG somewhat, which was again increased by BL treatment for 90 min. The wild-type sample or the transgenic line expressing BAK1-GFP alone did not show any significant nonspecific immunoprecipitation of BAK1-GFP by anti-Flag antibody under the conditions of the experiment.

In Vivo Phosphorylation of BRI1 and BAK1 on Thr Residues Is BL Dependent

Based on a phosphatase susceptible gel mobility shift of BRI1 extracted from BL-treated tissue, it was previously demonstrated in a general way that BRI1 phosphorylation is likely to be BR dependent in vivo (Wang et al., 2001). To more specifically examine the effect of BR levels on the in vivo phosphorylation status of Thr residues in BRI1 and BAK1, we used the same double transgenic experimental system described above, in conjunction with an antiphosphothreonine antibody that recognized the phosphorylated forms of the two proteins but showed no binding to unphosphorylated BRI1 and BAK1 kinase domains. Figures 1F and 1G show that in vivo phosphorylation of BRI1-Flag and BAK1-GFP on Thr residues was dramatically increased by BL treatment and that reduction of endogenous BL levels by BRZ treatment eliminated (BRI1-Flag) or greatly reduced (BAK1-GFP) Thr phosphorylation levels. Equal amounts of immunoprecipitated BRI1-Flag (Figure 1D) or BAK1-GFP (Figure 1C) were loaded in each case. Thus, most or all of the Thr residues that are phosphorylated in BRI1 and BAK1 result from activation of a BL-dependent signaling pathway. We could not find a

(H) ProQ Diamond stain, which recognizes phosphorylated Ser and Thr residues, binds to BRI1-Flag immunoprecipitated from plants with reduced endogenous BL, suggesting that at least one Ser residue is constitutively phosphorylated in vivo. Sypro Ruby is a general protein stain that shows loading levels.

(I) GST-BAK1-KD and Flag-BRI1-KD are recombinant cytoplasmic domains of BAK1 and BRI1 purified from bacteria and autophosphorylated in vitro. GST-mBAK1-KD and Flag-mBRI1-KD both have a K-to-E substitution in kinase subdomain II, resulting in complete inability to autophosphorylate in vitro. The phosphothreonine antibody recognizes only the phosphorylated form of BAK1. See Figure 6C for an identical result with BRI1. Similarly, ProQ Diamond recognizes only the phosphorylated form of BRI1.

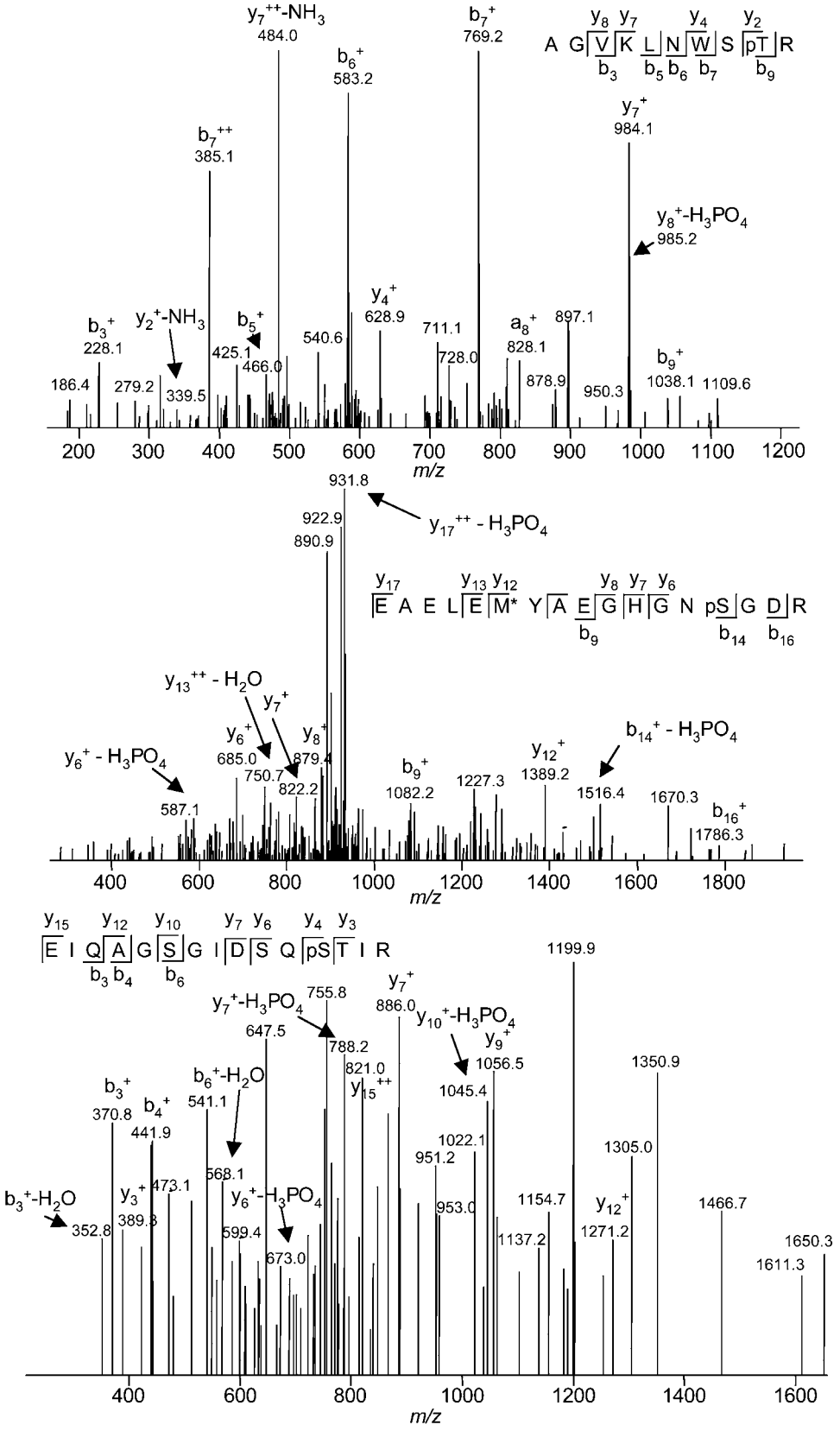

Figure 2. Ion Trap MS/MS Spectra Identifying BRI1 in Vivo Phosphorylation Sites.

commercially available antiphosphoserine antibody with the same specificity as the phosphothreonine antibody used in Figure 1. However, experiments with the Pro-Q Diamond stain (Molecular Probes, Eugene, OR), which recognizes both phosphorylated Ser and Thr residues, indicated that at least one Ser in BRI1 was constitutively phosphorylated at significant levels (Figure 1H). Whether the commercial antiphosphothreonine antibody recognizes all BRI1 phosphothreonine residues or only a subset was not determined. Thus, it is possible that a specific phosphothreonine not recognized by the antibody because of sequence context might also contribute to the constitutive phosphorylation observed with Pro-Q Diamond staining.

BRI1 Is Phosphorylated on Multiple Ser and Thr Residues in Vivo

To identify in vivo autophosphorylation sites, transgenic plants expressing a C-terminal fusion of full-length BRI1 followed by the short Flag epitope were grown in shaking liquid culture for 11 d and treated with BL for 90 min before harvest. Total membrane proteins were extracted in the presence of phosphatase inhibitors, solubilized and immunoprecipitated with anti-Flag antibody linked to agarose beads as previously described (Li et al., 2002). After SDS-PAGE, the BRI1-Flag band was excised, digested with trypsin, and subjected to ion trap or QTOF LC/MS/MS analysis, with or without immobilized metal affinity chromatography (IMAC) to enrich for phosphorylated peptides. MS/MS spectra of the phosphorylated peptides are shown in Figures 2 and 3, and the identified phosphorylated peptides are listed in Table 1. These indicated sites of phosphorylation elicited the highest SEQUEST (Eng et al., 1994) or Mascot (Perkins et al., 1999) scores based on the generated b and y product ions and were corroborated by manual inspection of the data. The compilation of all MS/MS data covered >91% of the BRI1 cytoplasmic domain sequence and unambiguously identified S-838, S-858, T-872, and T-880 in the juxtamembrane region, T-982 in kinase subdomain VIa, and S-1168 in the C-terminal region as true in vivo phosphorylation sites. All of these, except T-880, were previously identified as confirmed or possible in vitro autophosphorylation sites of the recombinant BRI1 cytoplasmic domain (Oh et al., 2000).

Based on previous in vitro results, it was expected that T-842 and T-846 might also be phosphorylated in vivo, in addition to up to three sites of phosphorylation in the activation loop of subdomains VII/VIII, spanning residues 1027 to 1056 of BRI1 (Oh et al., 2000). However, specific sites of phosphorylation in these regions were not identified from the MS/MS spectra acquired from the ion trap or QTOF analyses based on SEQUEST or Mascot searching algorithms, respectively. To investigate phosphorylation in these two regions further, extracted ion chromatograms from the MS data of several ion trap LC/MS/MS runs were generated for each possible tryptic peptide spanning the areas of interest based on calculations using various charge states, biochemically feasible phosphorylation stoichiometries, alkylated Cys residues, and the presence of Met sulfoxide as a result of Met oxidation that occurs during electrophoresis.

The peptides matching these criteria that displayed a detectable signal are listed in Table 2, which contains the calculated neutral mass and the deconvoluted mass for each observed precursor ion. Peptides displaying multiply charged precursor ions were detected in the same MS spectrum and at the same retention time. Manual inspection of data for each peptide identified by this method indicated that approximately one-half of the detected precursor ions were trapped and subjected to collision-induced dissociation (CID). However, the resulting fragmentation did not generate enough b and y product ions of sufficient intensity for positive identification using SEQUEST. This was particularly true for the precursor ions that contained four protons, $[M+4H]^{4+}$ because (1) most of the b and y ions would have mass-to-charge (*m/z*) ratios > 2000 and remain undetectable by the ion trap as a result of the predefined acquisition parameters, and (2) the SEQUEST algorithm lacks the capability of matching product ions generated from $[M+4H]^{4+}$ precursor ions. Based on the data of Table 2, the region 842-TANNTNWKLTGVK-854 appears to be singly or doubly (but not triply) phosphorylated, indicating that at least two of the Thr residues are phosphorylated in vivo. However, the detected precursor ions of $[M+3H]^{3+}$ and $[M+4H]^{4+}$ of the oxidized peptide 825-EAELEM*YAEGHGNSGDRTANNTNWKLTGVK-854 containing four phosphates were observed, suggesting that T-851 can also be phosphorylated in vivo under some circumstances. A similar analysis shows that the peptide 1033-LMSAMDTHLSVSTLAGTPGYVPPEYYQSFR-1062, containing all of the six Thr and Ser residues within the BRI1 activation loop, can be phosphorylated on up to three sites in vivo, which is consistent with our previous findings of autophosphorylation of three residues of the activation loop of the BRI1 kinase domain in vitro (Oh et al., 2000).

Figure 2. (continued).

Eleven-day-old light-grown Arabidopsis plants expressing a full-length BRI1 gene with a C-terminal Flag epitope were treated with 0.1 μM BL, and BRI1-Flag was immunoprecipitated with anti-Flag antibody linked to agarose beads. The protein was PAGE purified and in-gel digested with trypsin, and the resulting peptides were extracted and analyzed by LC/MS/MS using a capillary LC system coupled directly to a LCQ Deca ion trap mass spectrometer. Each MS/MS spectrum is a collection of ions produced by collision-induced dissociation of the intact peptide. The fragmentation preferentially occurs at peptide bonds to generate N-terminal fragments (b ions) and C-terminal fragments (y ions) at specific *m/z* ratios and intensities that provide information regarding amino acid sequence and sites of modification as indicated by vertical lines between residues of the peptide sequence. The predominant b and y product ion peaks are labeled accordingly with the subscripts denoting their position in the identified peptide and the superscripts of $+$ and $++$ indicating singly and doubly protonated ions, respectively. Product ions eliciting neutral mass losses of H_2O, NH_3, and H_3PO_4 are also indicated. Identified phosphoseryl and phosphothreonyl resides are denoted as pS and pT, respectively. Met sulfoxide residues (oxidized Met) are labeled as M*. Analysis of y and b ion fragmentation patterns with SEQUEST showed that S-838, T-982, and S-1168 were phosphorylated in vivo.

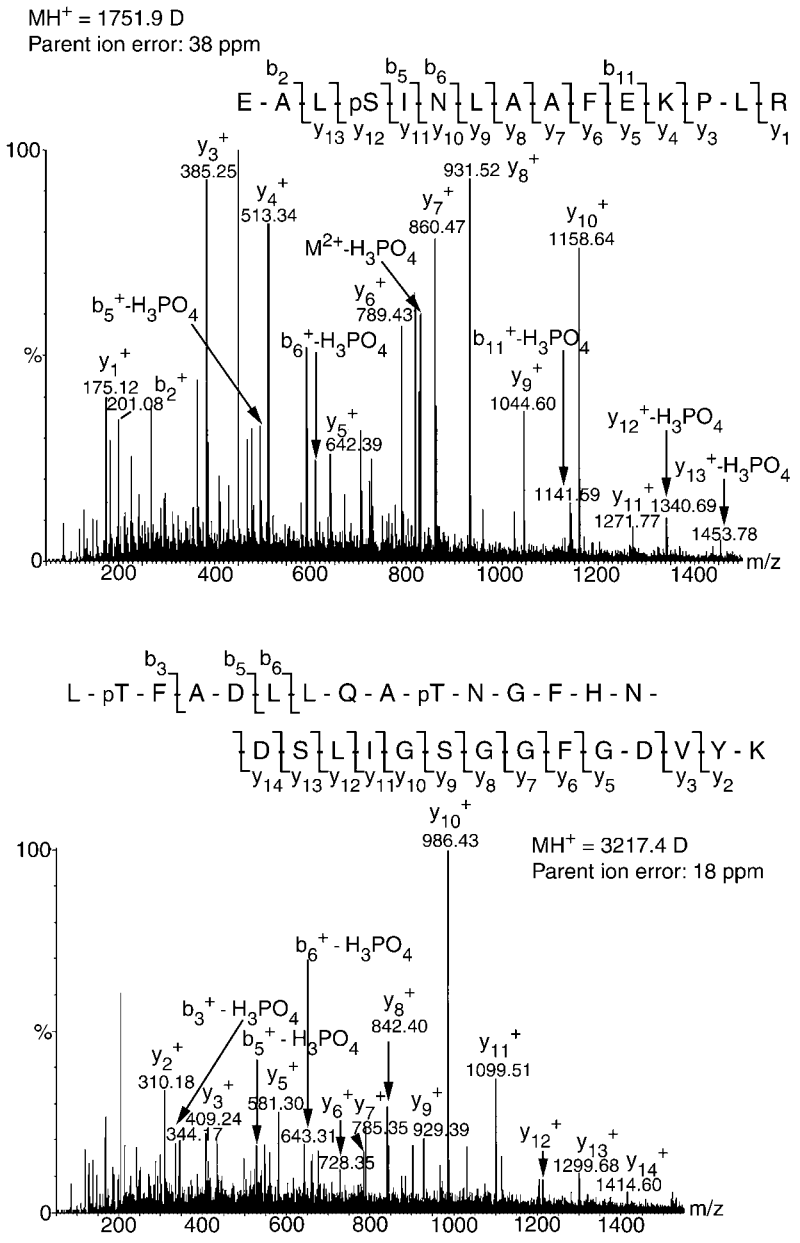

Figure 3. QTOF MS/MS Spectra Identifying BRI1 in Vivo Phosphorylation Sites.

BRI1-Flag was immunoprecipitated from Arabidopsis plants as described in Figure 2. The protein was SDS-PAGE purified and in-gel digested with trypsin, and the resulting peptides were extracted and analyzed by LC/MS/MS analysis on a capillary LC system coupled directly to a Waters Q-ToF Ultima mass spectrometer (Milford, MA). The measured mass (D) of the singly protonated peptide and the corresponding mass measurement accuracy (ppm) are reported above each spectrum. The ion product spectrum corresponding to fragmentation of each singly charged peptide is shown. Prominent b and y ions are labeled as in Figure 2, including neutral loss of H_3PO_4 (98 D) from phosphorylated peptides as indicated. Analysis of y and b ion fragmentation patterns with Mascot showed that S-858, T-872, and T-880 were phosphorylated in vivo.

The in-gel trypic digestion used here might be a limiting factor because of difficulties in digestion at the trypic sites in the juxtamembrane and activation loop regions shown in Table 2, or the peptide extraction efficiencies from the gel of these fragments may be altered. However, the MS data based on mass measurement at unit resolution of the precursor ions for the peptides listed in Table 2 indicates that phosphorylation is taking place, and these data are supported by the preponderance of in vitro evidence that suggests that these regions are multiply phosphorylated (Oh et al., 2000). Thus, we have shown compelling

Table 1. Identification of Six in Vivo Phosphorylation Sites (S-838, S-858, T-872, T-880, T-982, and S-1168) of Immunoprecipitated BRI1-Flag by Ion Trap or QTOF LC/MS/MS

Peptide[a]	Calculated Mass[b]	Measured Mass[c]	Charge State	Score	Ions[d]
K.EAELEM*YAEGHGNpSGDR.T	1960.9	1960.2	2	2.16[e]	14/32
K.EAELEM*YAEGHGNpSGDR.T		1960.7	2	69[f]	16/32
K.EAELEM*YAEGHGNpSGDR.T		1960.9	2	1.75[e]	14/32
K.EALpSINLAAFEKPLR.K	1751.9	1752.8	2	89[f]	16/28
K.LpTFADLIQApTNGFHNDSLIGSGGFGDVYK.A	3218.3	3219.5	3	52[f]	15/56
K.AGVKLNWSpTR.R	1211.3	1211.1	2	1.79[e]	7/18
K.EIQAGSGIDSQpSTIR.S	1641.6	1640.9	2	2.02[e]	13/28

[a] The amino acid residues appearing before and after the periods correspond to the residues proceeding and following the peptide in the protein sequence. Met sulfoxide is denoted as M*; phosphoseryl and phosphothreonyl residues are denoted as pS and pT, respectively.
[b] Average peptide mass.
[c] Deconvoluted mass determined from the observed *m/z* at the reported charge state.
[d] The total number of b and y ions (identified/theoretical).
[e] SEQUEST cross-correlation score (Xcorr) of the peptide is based on the fit of the ion trap MS/MS data to the theoretical distribution of ions produced for the peptide.
[f] Mascot score for QTOF analysis.

evidence for at least 11 sites of in vivo phosphorylation in BRI1 (summarized in Figure 4), six of which are unambiguously identified by MS/MS, and five of which are localized to specific peptides based on detection of multiply charged precursor ions and chromatographic retention.

Specific Activation Loop Residues Are Highly Conserved among Arabidopsis LRR RLKs

As mentioned previously, phosphorylation of one to three residues in the activation loop of the kinase domain is often required for ligand-induced kinase activation. Most kinases have an invariant Asp in subdomain VIb (D-1009 in BRI1), which is required for catalytic activity, and many, the so-called RD kinases, also have an Arg immediately upstream of this Asp residue. In animal systems, those kinases that require autophosphorylation of the activation loop for kinase activity are predominately of the RD class, where the phosphorylated, negatively charged amino acid of the activation loop is thought to interact with the positively charged Arg to provide the proper spatial environment for substrate access to the catalytic Asp (Johnson et al., 1996). BRI1 and many other plant RLKs also contain an Arg at this position (R-1008 in BRI1). Genetic analysis also points to the functional importance of this region because numerous mutations in plant RLKs fall within the activation loop (Lease et al., 1998), including *bri1*-104 and *bri1*-115 (Li and Chory, 1997). Furthermore, biochemical analysis of both plant RD-type soluble kinases and RLKs has provided several examples of the critical importance of phosphorylation of the activation loop for in vitro kinase activity and/or in vivo kinase function (Sessa et al., 2000; Shah et al., 2001; Guo et al., 2004; Yoshida and Parniske, 2005). With a conserved mechanism of activation, it would be expected that there is a high degree of sequence conservation in the activation loop among RLKs, particularly at specific residues that must be phosphorylated for activation to occur. Figure 5 shows that by manually examining a PileUP alignment of the entire 610-member RLK family (Shiu and Bleecker, 2001), 82.9% of Arabidopsis RLKs have a Thr or Ser at the position equivalent to T-1049 in BRI1, whereas 62.8% have such a residue at the position equivalent to BRI1 S-1044. When looking specifically at LRR RLKs, 72.8% have S or T at the BRI1 T-1049 position, and 63.6% have these residues at the BRI1 S-1044 position. Residues aligning with BRI1 T-1039 and S-1042 have a conserved S or T in ~45% of all RLKs and LRR RLKs, whereas residues aligning with BRI1 S-1035 and T-1045 are much less conserved.

Direct sequence inspection shows that RD-type kinases comprise 121 out of 213 (56.8%) of all Arabidopsis LRR RLKs. Interestingly, when one compares an alignment of BRI1 with RD versus non-RD LRR RLKs, a very different picture of sequence conservation in the activation loop is apparent. More than 99% of RD LRR RLKs have an S or T at the position aligning with BRI1 T-1049, whereas only 30.4% of non-RD LRR RLKs have S or T at the equivalent position. Similarly, for the conserved residues equivalent to BRI1 T-1039, S-1042, and S-1044, S or T residues occur at least 4.7-fold more often in RD versus non-RD LRR RLKs. By contrast, the less conserved residues aligning with BRI1 S-1035 and T-1045 have an S or T at the equivalent position more often in non-RD LRR RLKs than in RD kinases. Thus, in RD-type LRR RLKs, a Ser or Thr residue is very often found in positions equivalent to BRI1 T-1049, S-1044, T-1042, and T-1039, whereas in non-RD kinases, Ser and Thr residues are much less conserved at these positions. Figure 5C illustrates the high conservation of residues corresponding to these four positions among twelve Arabidopsis RD LRR RLKs of known function.

To examine activation loop phosphorylation of RD LRR RLKs further, GST-BAK1 (Li et al., 2002) was autophosphorylated in vitro and subjected to ion trap LC/MS/MS analysis. Table 3 shows that three Thr residues lying within the activation loop of BAK1, T- 446, T-449, and T-455, were phosphorylated. These residues correspond to T-1039, S-1042, and T-1049 in the activation loop of BRI1. GST-BAK1 residue S-290, at the beginning of kinase subdomain I, was also found to be phosphorylated in vitro by this analysis.

Table 2. Additional Phosphopeptides Identified from Immunoprecipitated BRI1-Flag: Determination of in Vivo Phosphorylation Stoichiometry of Juxtamembrane and Activation Loop Tryptic Peptides Based on Measured Precursor Peptide Mass

Peptide[a]	Calculated Mass[b]	Measured Mass[c]	Charge State	No. of HPO_3
R.TANNTNWKLTGVK.L	1446.6	n.d.[d]	–	0
	1526.6	1526.6	2	1
	1606.5	1606.3	2	2
	1686.5	n.d.	–	3
K.EAELEMYAEGHGNS-GDRTANNTNWK.L	2794.9	n.d.	–	0
	2874.8	2875.0	3	1
	2954.8	n.d.	–	2
	3034.8	3034.8	2	3[e]
K.EAELEMYAEGHGNSGD-RTANNTNWKLTGVK.E	3293.5	3293.4	4	0
	3373.5	n.d	–	1
	3453.4	n.d	–	2
	3533.4	3534.0	4	3
	3613.4	n.d.	–	4
K.EAELEM*YAEGHGNSGD-RTANNTNWKLTGVK.E	3309.5	3309.3	3	0
	3389.5	n.d	–	1
	3469.4	n.d	–	2
	3549.4	3549.3	4	3
	3629.4	3629.7	3	4
	3629.4	3629.7	4	4
R.LMSAMDTHLSVSTLAG-TPGYVPPEYYQSFR.C	3319.8	n.d.	–	0
	3399.8	3399.1	2	1
		3400.4	4	1
	3479.7	3480.2	2	2
		3480.0	4	2
	3559.7	3559.2	2	3
		3561.6	3	3
		3561.2	4	3
R.VSDFGMARLMSAMD-THLSVSTLAGTPGYV-PPEYYQSFRC‡STK.G	4660.3	n.d.	–	0
	4740.3	4740.6	3	1
		4742.0	4	1
	4820.3	4820.0	4	2
	4900.3	4899.6	3	3
		4898.8	4	3

[a] The amino acid residues appearing before and after the periods correspond to the residues proceeding and following the peptide in the protein sequence. Met sulfoxide is denoted as M* and carboxamidomethyl-Cys is denoted as C‡.

[b] Average peptide mass.

[c] Deconvoluted mass determined from the observed *m/z* at the reported charge state. The number of phosphorylation events was determined based on the measured peptide mass. Because of lack of precursor ion capture or inadequate CID after capture, the specific phosphorylated residue(s) could not be determined.

[d] Not detected.

[e] This phosphopeptide was only detected in the IMAC enriched sample.

Although a general activation mechanism of the kinase domain might be predicted in many plant RLKs based on conservation of phosphorylated residues in the activation loop, RLKs function in many diverse physiological processes, and mechanisms for transducing signals to pathway-specific cytoplasmic components are also required. Autophosphorylation of less conserved juxtamembrane and C-terminal regions to create docking sites for RLK substrates may be one way to achieve this specificity. A sequence alignment of the cytoplasmic domains of 213 Arabidopsis LRR RLKs (Figure 5B) shows that outside of the catalytic kinase domain, Ser or Thr residues are highly conserved only in positions equivalent to BRI1 T-872 and T-880 in the juxtamembrane region. Other phosphorylation sites in the juxtamembrane and C-terminal regions of BRI1 are not conserved within the LRR RLK family.

Site-Directed Mutagenesis of Identified and Predicted BRI1 Phosphorylation Sites Affects Kinase Function

The functional significance of each of the identified and predicted phosphorylation sites in BRI1 was assessed by site-directed mutagenesis of each specific Ser or Thr to Ala followed by biochemical analysis in vitro and testing for the ability of the altered construct to rescue the weak *bri1-5* BR-insensitive mutant in planta. Two sets of mutated constructs were generated for each of 17 sites: recombinant cytoplasmic domains (amino acids 815 to 1196) with a Flag N-terminal tag and the full-length BRI1 gene with a C-terminal Flag tag in a pBIB-Hyg binary plant transformation vector (Becker et al., 1992), driven by the BRI1 native promoter. The 17 sites covered all six unambiguously identified in vivo sites, the predicted juxtamembrane sites T-842 and T-846, the four most conserved activation loop sites (S-1044 and T-1045 were mutated in the same construct for convenience), and several other sites previously predicted to be potentially phosphorylated in vitro (Oh et al., 2000).

For biochemical function, we assessed the effect of mutagenesis on autophosphorylation of the BRI1 cytoplasmic domain in vitro and on phosphorylation of a synthetic peptide (BR13) containing the previously determined consensus sequence for optimum BRI1 substrate phosphorylation (Oh et al., 2000). Figure 6 shows that the mutations T-1049-A and either S-1044-A or T-1045-A in the kinase domain activation loop nearly abolished kinase activity, with respect to both autophosphorylation and peptide substrate phosphorylation. Interestingly, mutations T-1039-A and S-1042-A had more effect on substrate phosphorylation than autophosphorylation. Juxtamembrane substitutions at residue 838, 842, 846, or 858 did not result in appreciable differences in autophosphorylation compared with Flag-BRI1-KD (kinase domain), but resulted in from 74 to 88% reduction in phosphorylation of the BR13 synthetic peptide when compared with Flag-BRI1-KD. Similarly, substitutions at residues 1168, 1172, 1179/1180, and 1187 in the C-terminal region had little observable effect on autophosphorylation but reduced BR13 peptide phosphorylation by 47 to 74%. Kinetic analysis of T-842-A and S/T-1179/1180-A (Figure 7) was consistent with a reduced enzyme catalytic efficiency caused by these mutations because V_{max}:K_m ratios were 11.8 and 30.5% that of

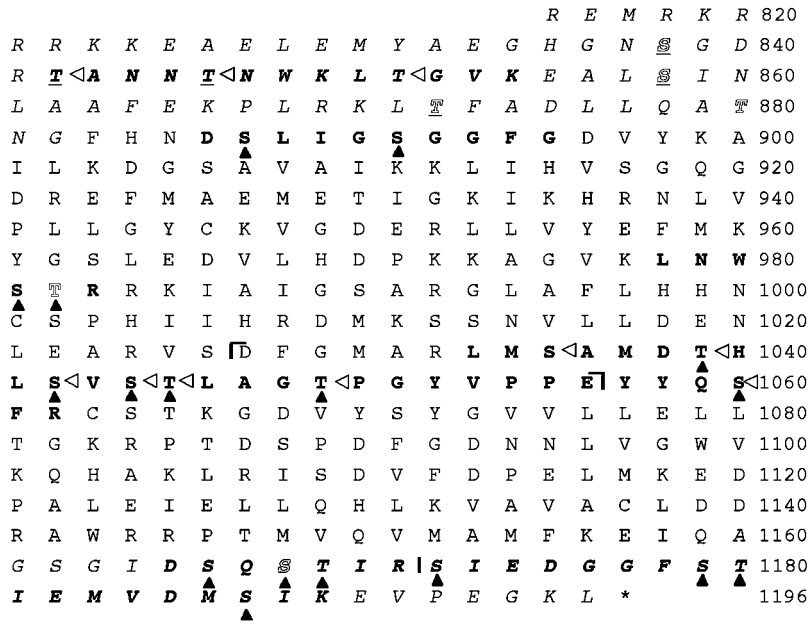

Figure 4. Summary of BRI1 Phosphorylation Sites.

The juxtamembrane region and C-terminal region are italicized. The six confirmed sites of in vivo phosphorylation are outlined, and the five confirmed sites of in vitro phosphorylation (Oh et al., 2000) are underlined. Phosphorylated peptides with ambiguity in the specific residues are indicated in bold, with open triangles showing possible in vivo sites and closed triangles possible in vitro sites. The activation loop is marked with brackets and the peptide beginning with LMSAM is phosphorylated on three of the Ser or Thr residues in vivo. The peptide beginning with DTHLS is phosphorylated on three Ser or Thr residues in vitro. The peptide TANNTNWKLTGVK is phosphorylated on two of the three marked residues in vivo. All of the remaining peptides in bold are phosphorylated on only one of the indicated residues in vitro and on the specific residues outlined in vivo.

Flag-BRI-KD, respectively. These findings are consistent with the model that autophosphorylation of the activation loop is required for general kinase activity, whereas autophosphorylation of juxtamembrane and C-terminal residues either generates docking sites for specific downstream substrates or affects catalytic activity toward those substrates.

Quite unexpectedly, we found that mutation T-872-A resulted in an ~10-fold increase in peptide substrate phosphorylation (Figure 6B). There was also a prominent shift in mobility of this mutant on SDS-PAGE, suggesting a pronounced difference in phosphorylation state. Whereas the autoradiograph in Figure 6A shows an apparent reduction in autophosphorylation of T-872-A, protein gel blot analysis with an antiphosphothreonine antibody revealed that T-872-A autophosphorylated to a very high degree within *Escherichia coli* during recombinant protein production, allowing less uptake of [γ-^{32}P]ATP during the kinase assay in vitro (Figure 6C). None of the other constructs showed this hyperphosphorylation in *E. coli* (data not shown). Kinetic analysis (Figure 7) confirmed that the K_m of T-872-A for BR13 was reduced approximately twofold compared with the wild type, whereas V_{max} increased ~10-fold, producing an 18-fold increase in V_{max}:K_m. If reflected in vivo, T-872 might be a negative regulatory site when phosphorylated, and removal of this phosphate could lead to activation of the kinase and increased recognition of specific substrates. Interestingly, T-872 was one of two juxtamembrane sites that were highly conserved in an alignment of RD LRR RLKs, suggesting phosphorylation at this site might be a general mechanism among these kinases.

Specific Ser and Thr Activation Loop Residues Are Required for BRI1 Signaling in Planta

The *bri1-5* mutant is a weak allele that shows intermediate dwarfism and a smaller rosette size because of a C69Y amino acid substitution in the extracellular domain of BRI1 (Noguchi et al., 1999). The number and location of phosphorylation sites within BRI1 coupled with the biochemical analysis presented above suggest that phosphorylation of specific Ser and Thr residues may control kinase activation and recognition of downstream signaling components. Altering these specific Ser and Thr residues individually may result in a complete or partial loss of ability to rescue *bri1-5*, depending on whether the mutation results in loss of kinase activity or inability to bind to specific downstream components. Four mutations in the juxtamembrane region, four in the activation loop, and two in the C-terminal region were compared for their ability to rescue *bri1-5* with a wild-type construct and a kinase-inactive mutant generated by a K-911-E substitution of the invariant residue in subdomain II (Oh et al., 2000). In each case, 50 independent transgenic lines were evaluated visually for phenotype compared with untransformed Wassilewskija-2 (Ws-2) wild type and the *bri1-5* mutant. Two individuals that represented the typical phenotype among the 50 lines were selected for each mutant, in addition to one individual with a divergent phenotype (Figure 8). Young leaves from approximately the same position in the rosettes of these individuals of the same age, grown under identical conditions, were harvested for total protein and DNA extraction. Transgene

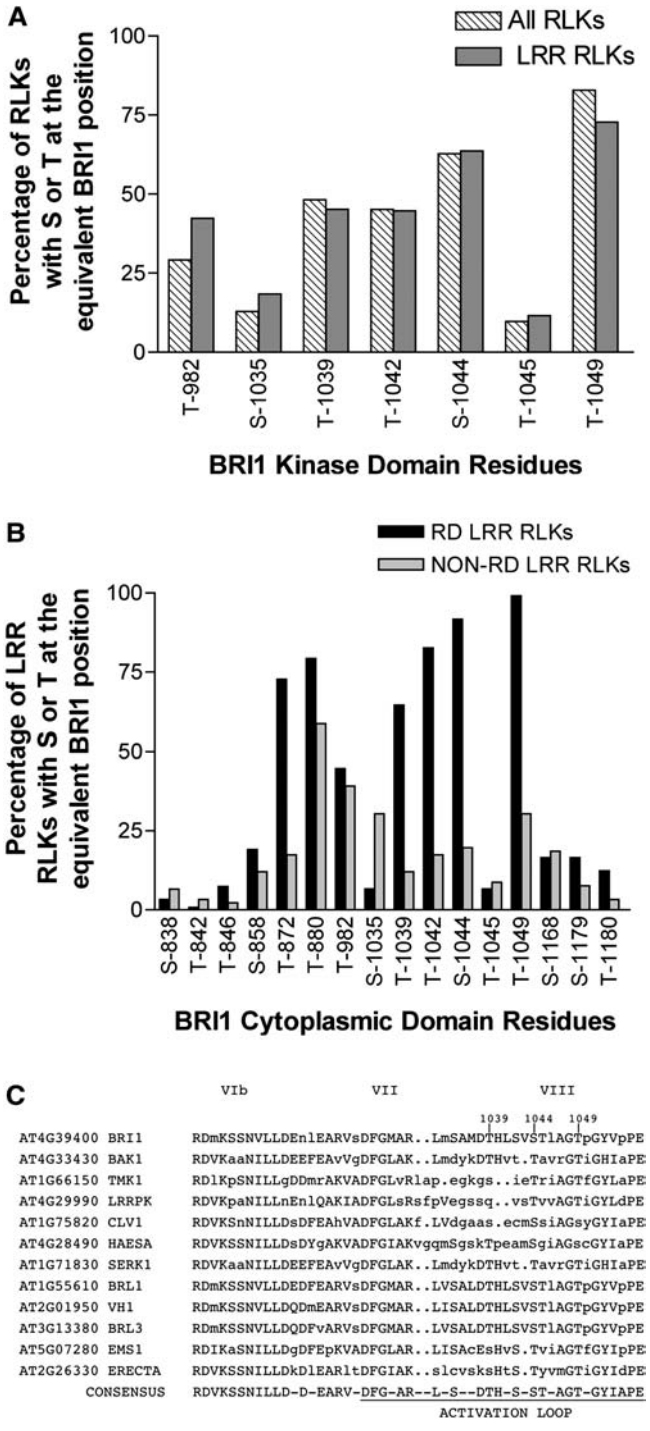

Figure 5. Conserved Ser and Thr Residues in the Arabidopsis RLK Family Corresponding to Possible BRI1 Phosphorylation Sites.

(A) A PileUP protein alignment of the kinase domains of all 610 Arabidopsis RLKs (Shiu and Bleecker, 2001) was visually examined for the presence of Ser or Thr residues at specific sites in the alignment corresponding to the indicated BRI1 residues. A subset of 217 putative LRR RLKs was tabulated separately.

(B) The intracellular domains of 121 Arabidopsis LRR RLKs containing an Arg immediately preceding the invariant Asp in the catalytic site of subdomain VI (RD kinases) were aligned with ClustalW, and the number of Ser and Thr residues occurring in the positions corresponding to the indicated BRI1 residues were tabulated. A similar analysis was performed with 92 non-RD Arabidopsis LRR RLKs.

(C) Specific activation loop residues of RD LRR RLKs are highly conserved. PileUp was used to align sequences in 12 LRR RLKs (RD-type kinases) from the RD in subdomain VIb to the invariant E in subdomain VIII. Note the very high conservation of Ser or Thr residues at positions corresponding to BRI1 T-1039, S-1044, and T-1049.

expression was monitored by protein gel blot analysis with an anti-Flag antibody, and expression levels of endogenous BRI1 were determined by competitive RT-PCR using an in vitro synthesized internal RNA standard corresponding to the amplified BRI1 region but with a 53-nucleotide deletion.

Figure 8 shows that the wild-type BRI1-Flag construct was capable of rescuing *bri1-5* to the typical Ws-2 phenotype and that rescue was correlated with expression of the transgene. In the case of the K-911-E mutant, no rescue of *bri1-5* was observed; in fact, high levels of transgene expression led to a phenotype smaller than *bri1-5*, whereas lack of expression resulted in plants the same size as untransformed *bri1-5*, suggesting a dominant negative effect, which was also observed previously by overexpressing a K-317-E mutant of BAK1 in *bri1-5* (Li et al., 2002). Individual substitutions in the juxtamembrane or C terminus did not have an obvious affect on *bri1-5* rescue, where high levels of transgene expression resulted in plants as large as Ws-2 or the wild-type BRI1 transgenics, whereas lines that did not express the transgene remained dwarfed. The smaller lines tested in each of these mutants all appeared to result from cosuppression of endogenous BRI1, as determined by competitive RT-PCR, which resulted in an extreme dwarf phenotype similar to *bri1* null alleles.

By contrast, mutations in the activation loop dramatically affected ability of the construct to rescue *bri1-5*. Where the transgene was expressed, T-1039-A and S-1042-A both showed a phenotype that was intermediate between *bri1-5* and Ws-2, consistent with their attenuating affect on both autophosphorylation and substrate phosphorylation in vitro. Also consistent with their nearly complete loss of kinase activity in vitro, T-1049-A and S/T-1044/45-A were incapable of *bri1-5* rescue in any of the 50 independent transgenic lines examined for each. In fact, Figure 8 shows that high levels of S/T-1044/45-A expression (in the absence of cosuppression) resulted in plants smaller than the K-911-E kinase-inactive mutant, again suggesting a significant dominant negative effect. In the case of T-1049-A, the smallest plant appeared to be due to cosuppression, but a threshold level of transgene expression resulted in a plant of approximately the same size as the K-911-E mutant, but smaller than untransformed *bri1-5* itself, again suggesting a dominant negative effect.

DISCUSSION

Rapid progress in BR signal transduction research has made this pathway one of the best understood in plants, but the molecular mechanisms of BRI1/BAK1 heterodimerization and the identification of specific in vivo phosphorylation sites that lead to kinase

Table 3. Identification of Four in Vitro Phosphorylation Sites (S-290, T-446, T-449, and T-455) of GST-BAK1 by Ion Trap LC/MS/MS

Peptide[a]	Calculated Mass[b]	Measured Mass[c]	Charge State	Score[d]	Ions[e]
R.ELQVASDN-FpSNKN-ILGR.G	1985.3	1986.1	2	2.29	13/32
K.LM*DYKDp-THVTTAVR.G	1745.7	1746.9	2	4.20	18/26
K.DTHVpTTAVR.G	1080.0	1080.1	2	2.11	13/16
R.GpTIGHIAPEY-LSTGK.S	1626.4	1624.7	3	2.00	20/56

[a] The amino acid residues appearing before and after the periods correspond to the residues proceeding and following the peptide in the protein sequence. Met sulfoxide is denoted as M*; phosphoseryl and phosphothreonyl residues are denoted as pS and pT, respectively.
[b] Average peptide mass.
[c] Deconvoluted mass determined from the observed *m/z* at the reported charge state.
[d] SEQUEST cross-correlation score (Xcorr) of the peptide is based on the fit of the ion trap MS/MS data to the theoretical distribution of ions produced for the peptide.
[e] The total number of b and y ions (identified/theoretical).

activation and substrate recognition in response to BR perception have not been previously reported for these LRR RLKs. We demonstrate here that the amount of BAK1-GFP coimmunoprecipitating with BRI1-Flag, and by inference the heterodimerization of BRI1 and BAK1 in vivo, is significantly affected by BL levels. However, coimmunoprecipitation of BRI1 and BAK1 was detectable at low levels in +BRZ and −BL plants, suggesting that ligand-independent heterodimerization of the two is also possible.

When expressed together in yeast cells, BRI1 and BAK1 coimmunoprecipated in the absence of BL treatments, indicating that the two LRR RLKs have some affinity for each other in the absence of ligand (Nam and Li, 2002). Moreover, the level of heterodimerization of BRI1 and BAK1 observed in protoplasts by FLIM analysis was not augmented by BL treatment, although endogenous levels of BRs in the cells were not depleted with BRZ in that study and thus could have affected the observed association between the two RLKs (Russinova et al., 2004). It is also possible that the protoplast system of FLIM analysis and our whole plant conditions of growth cannot be directly compared with respect to the mechanism of ligand-dependent or -independent BRI1/BAK1 association. In any case, it is likely that both ligand-dependent and ligand-independent heterodimerization of BRI1 and BAK1 occurs in planta, as has been observed for mammalian RTKs and TGF-β receptor Ser/Thr kinases (Massague, 1998; Schlessinger, 2002; Yu et al., 2002).

After ligand-dependent receptor oligomerization, the next step in the classical animal model of receptor kinase action is phosphorylation of the cytoplasmic domain(s) of one or more of the receptor components. We show here that the phosphorylation of both BRI1 and BAK1 in vivo, at least on some Thr residues, is highly BL dependent. Ser phosphorylation was not detected by this assay, but use of the phosphoamino acid–specific dye, Pro-Q Diamond, under the same experimental conditions with appropriate controls suggested that at least one Ser (and/or a phosphothreonine residue not recognized by the antibody) in the BRI1 cytoplasmic domain is constitutively phosphorylated in vivo. Early events in BR signaling have been compared with both TGF-β and RTK animal models. The TGF-β receptor complex is a heterotetramer of receptor pairs Tβ-RI and Tβ-RII. Tβ-RII homodimerizes in the absence of ligand and exhibits constitutive autophosphorylation (Massague, 1998). TGF-β binding by Tβ-RII induces formation of the heterotetramer with Tβ-RI and results in phosphorylation of Tβ-RI by Tβ-RII on specific Thr and Ser resides in the juxtamembrane domain (Huse et al., 2001). Once activated by phosphorylation, Tβ-RI propagates the signal by phosphorylating cytoplasmic substrates that translocate to the nucleus to help regulate the expression of TGF-β–responsive genes. By analogy with this model, it has been proposed that BRI1 binds BL exclusively, which promotes heterodimerization with BAK1 (Li et al., 2002). The recent discovery that BL binds directly to the 70–amino acid island in the extracellular domain of BRI1 (Kinoshita et al., 2005), a motif that BAK1 lacks, supports the TGF-β model in which Tβ-RII (analogous to BRI1) binds the ligand before associating with Tβ-RI (analogous to BAK1).

Our data are consistent with aspects of this model, including the ligand-promoted association of BRI1 and BAK1, the constitutive phosphorylation of BRI1 on Ser residues, and the BL-regulated phosphorylation of BAK1 in vivo. Interestingly, comparison of BAK1-GFP in vivo phosphorylation levels in lines expressing only BAK1-GFP with those in which BRI1-Flag is overexpressed with BAK1-GFP (Figure 1F) suggests that BRI1-Flag overexpression significantly enhances BAK1-GFP phosphorylation in the presence of BL. This suggests a prominent phosphorylation of BAK1 by BRI1, which is also consistent with the TGF-β model. However, our observed BL-dependent phosphorylation of BRI1 Thr residues in vivo, along with the reported transphosphorylation of BRI1 and BAK1 in vitro and in yeast cells (Nam and Li, 2002), more closely resembles the RTK model. In this model for BR signaling, BRI1 and BAK1 would occur primarily in monomeric form with a small proportion of ligand-independent heterodimers. Binding of BL shifts the equilibrium toward the heterodimer and leads to transphosphorylation of the BRI1 and BAK1 kinase domains, which then propagate the signal downstream by phosphorylating cytoplasmic substrates. To clarify the true nature of BRI1/BAK1 interaction, it will be necessary to examine specific phosphorylation sites and mechanisms in planta in both RLKs.

Here, we used a variety of LC/MS/MS procedures to identify a minimum of 11 in vivo phosphorylation sites for BRI1-Flag isolated from BL-treated plants. Sequence coverage of the BRI1 cytoplasmic domain was very high, but we cannot rule out additional phosphorylated sites of low stoichiometry that were not detected in our analysis. Multiple LC/MS/MS approaches were required to achieve a high level of sequence coverage, as has been observed in many phosphorylation studies (Loyet et al., 2005). The consistent identification of phosphorylated peptides containing S-838 in all of our LC/MS/MS experiments suggests that this residue is highly phosphorylated in vivo. A comprehensive analysis of relative phosphorylation levels of each identified site in response to BL and different growth conditions is currently

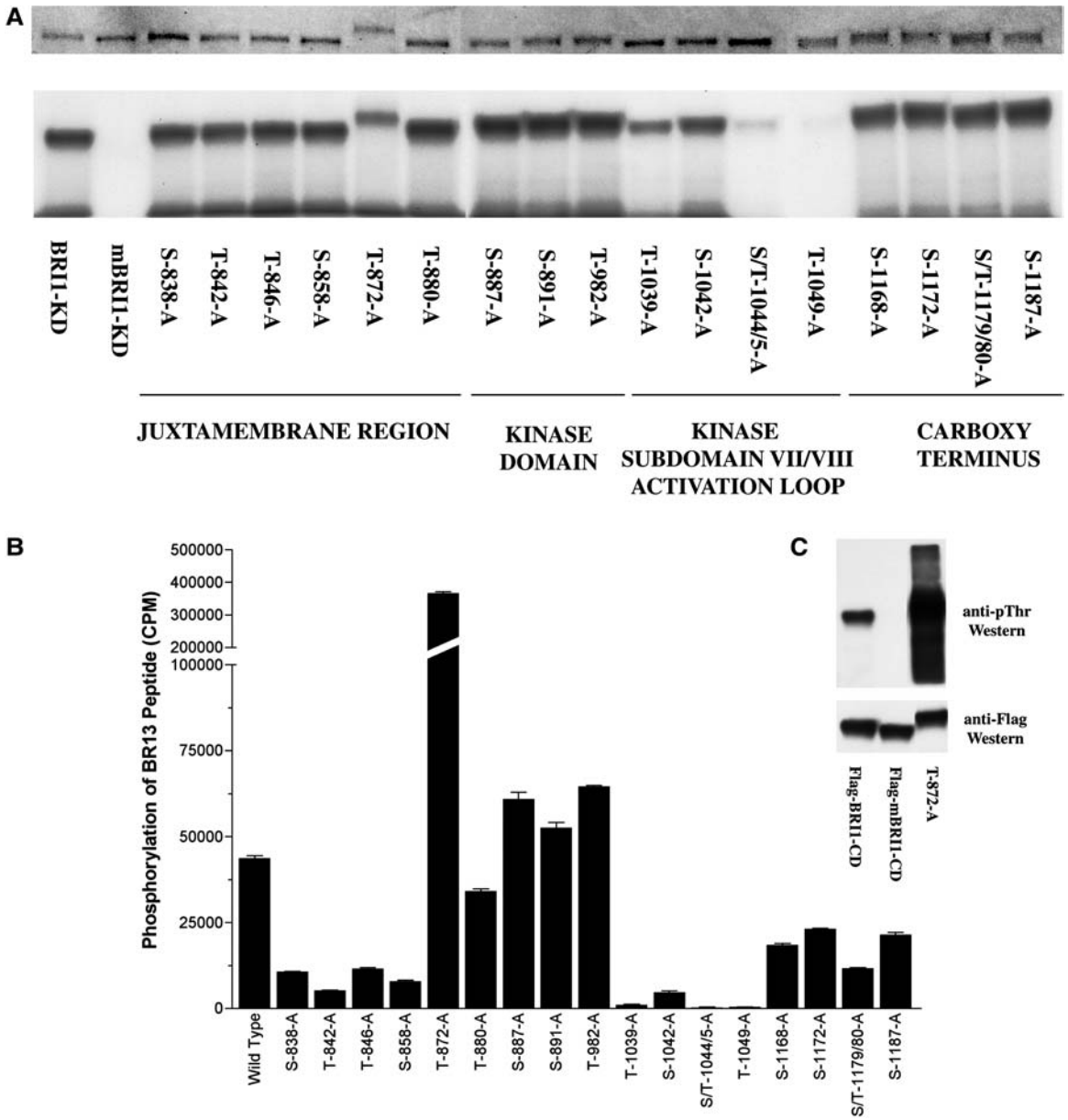

Figure 6. Effect of Mutating Specific Ser and Thr Residues of the BRI1 Cytoplasmic Domain on Autophosphorylation and Substrate Phosphorylation in Vitro.

(A) Autophosphorylation of recombinant Flag-BRI1-KD (wild type) and a range of mutants, including a kinase inactive mutant (mBRI1-KD) and constructs in which specific Ser and Thr residues were substituted with Ala by site-directed mutagenesis. Equal amounts of recombinant protein (as indicated by the stained gel in the top panel) were incubated with [γ^{32}P]ATP and separated by SDS-PAGE, followed by autoradiography (bottom panel). The experiment was repeated three times with consistent results.

(B) Phosphorylation of a synthetic peptide (BR13) containing the consensus sequence for optimum BRI1-KD substrate phosphorylation. Typically, a 40-μL reaction contained BRI1-KD or the indicated mutant protein (1.0 μg), 0.1 mM [γ-^{32}P]ATP (500 cpm/pmol), and synthetic peptide (100 μg mL^{-1}) in kinase buffer. Incorporation of ^{32}P into the synthetic peptide was quantified by binding to P81 phosphocellulose paper. Reactions were performed in triplicate. Error bars indicate SE.

(C) Hyperautophosphorylation of Flag-BRI1(T-872-A) in *E. coli*. Recombinant proteins were purified from *E. coli* with anti-Flag M_2 antibody attached to agarose beads, and 0.1 μg of recombinant protein was separated by SDS-PAGE. After transfer to polyvinylidene difluoride (PVDF) membranes, immunoblot analysis was performed with anti-Flag antibody to demonstrate equal protein transfer and antiphosphothreonine antibody to determine autophosphorylation levels. Note that the antibody was specific for the phosphorylated form of the protein (no signal with the kinase inactive mutant K-911-E, Flag-mBRI-KD) and that the high level of phosphosphorylation of the T-872-A mutation caused a mobility shift during SDS-PAGE.

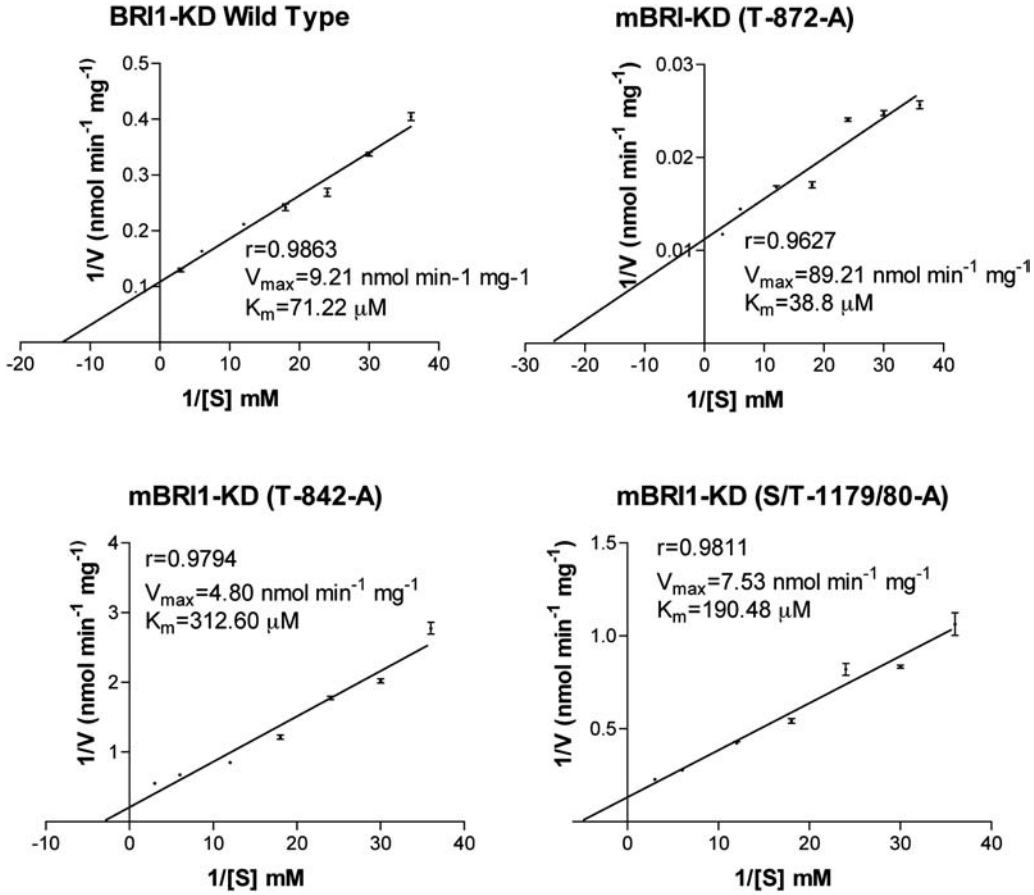

Figure 7. Effect of Mutating Specific Ser and Thr Residues of the BRI1 Cytoplasmic Domain on the Kinetics of BR13 Peptide Substrate Phosphorylation in Vitro.

Both K_m and V_{max} for BR13 were dramatically altered by substituting Ala for Ser or Thr at specific sites in the juxtamembrane or C-terminal regions of BRI1-KD. T-842-A and S/T-1179/80-A showed less catalytic activity, whereas T-872-A showed an ~10-fold increase in V_{max} and twofold reduction in K_m, indicating a much higher enzyme efficiency compared with the wild type.

underway using isotope-coded affinity tagging procedures (Qian et al., 2003). It was not surprising to find multiple phosphorylation sites in the juxtamembrane, kinase, and C-terminal domains of BRI1 based on our previous in vitro results (Oh et al., 2000) and on the observations accumulated in many other animal and plant receptor kinases (Wang et al., 1996; Baxter et al., 1998; Kalo and Pasquale, 1999; Binns et al., 2000; Huse et al., 2001; Guo et al., 2003). A phosphoproteomic analysis of Arabidopsis membrane proteins revealed multiple in vivo phosphorylation sites in >50 RLKs, with >75% of the identified sites occurring in the juxtamembrane and C-terminal regions and the remainder in the kinase domain, including the activation loop (Nuhse et al., 2004). The presence of multiple in vivo sites in all three cytoplasmic domains of plant RLKs suggests that, like the well-known mechanisms of animal RTK regulation, general kinase activation and specific downstream substrate recognition may be regulated by specific ligand-induced phosphorylation events in different RLK regions.

Our site-directed mutational analysis of confirmed or predicted BRI1 phosphorylation sites demonstrated that substituting specific Ser and Thr residues with Ala to prevent phosphorylation at that residue has differential effects on in vitro autophosphorylation versus phosphorylation of a peptide substrate. Most of the juxtamembrane and C-terminal residues are not highly conserved in alignments with other Arabidopsis RLKs, suggesting that phosphorylation at these sites might be involved in conferring BRI1-specific signaling properties (e.g., generation of docking sites for specific downstream cytoplasmic substrates), rather than a more general response of kinase activation. Several animal RTKs as well as Tβ-RI have been shown to play dual roles in juxtamembrane autophosphorylation (Huse and Kuriyan, 2002; Pawson, 2002). Besides creating docking sites for substrates with specific phosphopeptide binding motifs, the unphosphorylated juxtamembrane domain also serves to autoinhibit kinase function until relieved by ligand-dependent autophosphorylation at these residues (Hubbard, 2004). Based on in vitro biochemical data, BRI1 is unlikely to function in this manner because none of the juxtamembrane substitutions resulted in loss of general kinase activity as measured by in vitro autophosphorylation. Similary, autoinhibition of kinase activity

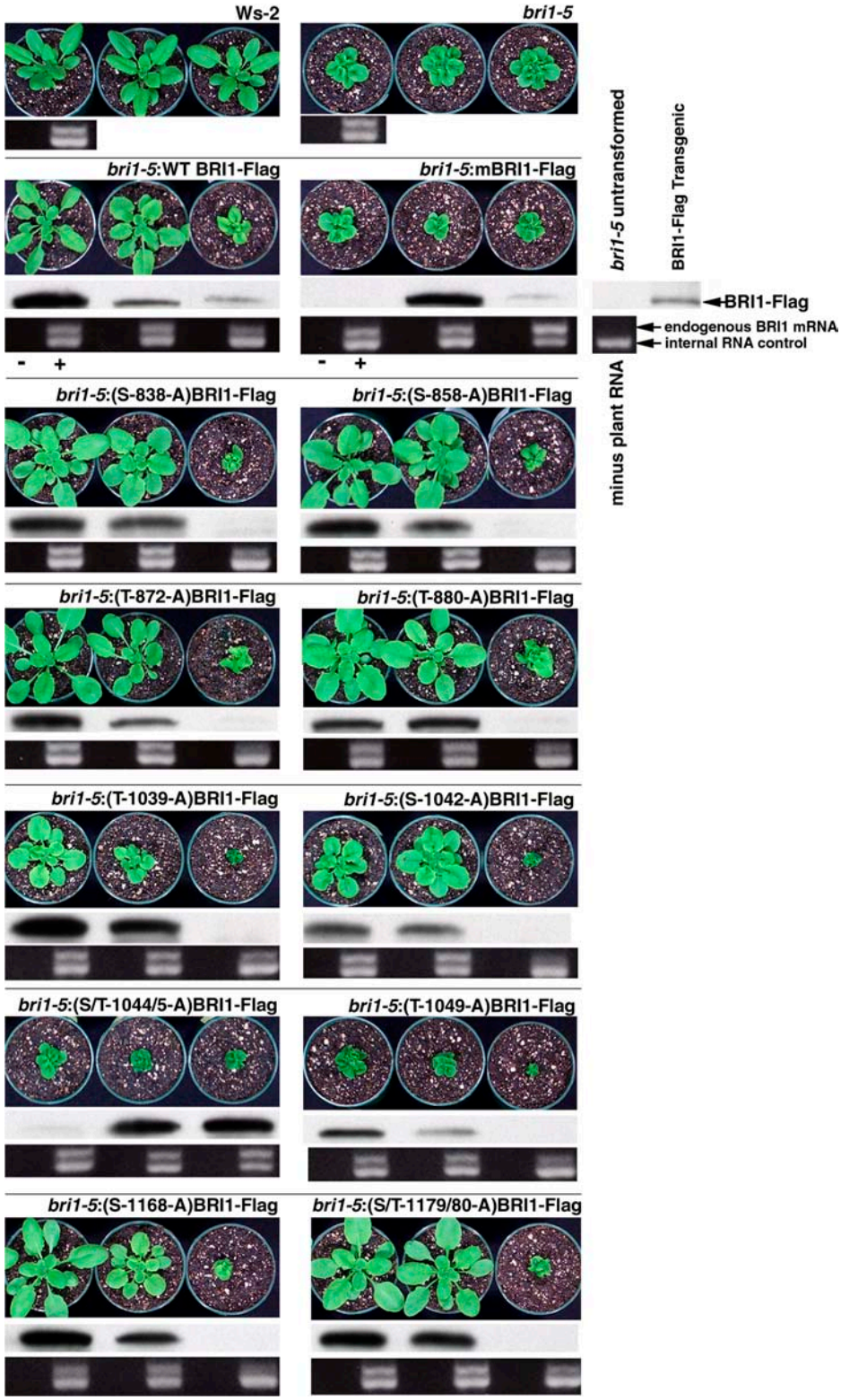

Figure 8. Effect of Mutating Specific Ser and Thr Residues of the BRI1 Cytoplasmic Domain on Rescue of the *bri1-5* Mutant.

Transgenic constructs contained 1699 bp of 5′ upstream BRI1 sequence (covering the BRI1 promoter and 5′ untranslated region), the entire coding region, and an in-frame C-terminal epitope tag (WT BRI1-Flag). A kinase-inactive version of the same construct was generated by a K-911-E mutation (mBRI1-Flag). Substitution of Ala for specific Thr or Ser residues within the wild-type construct are as indicated. Three independent transgenic lines for

has been observed by the unphosphorylated C-terminal region (Hubbard, 2004). By a similar argument presented for the juxtamembrane sites, the five C-terminal residues altered in BRI1 do not affect general kinase activity and thus are also unlikely, at least in vitro, to be autoinhibitory.

To test the effect of mutating specific Thr and Ser residues in the juxtamembrane and C-terminal regions on BRI1 function in vivo, we examined the extent to which each construct rescued the weak *bri1-5* mutant when compared with a wild-type construct. Because this is a simple gain-of-function assay, we examined multiple T1 transgenic lines with careful monitoring of the extent of trangene and endogenous BRI1 expression in each line. Of the four juxtamembrane and two C-terminal mutations examined, none appeared to affect the general ability of the transgene, when expressed at adequate levels from the native BRI1 promoter, to rescue the *bri1-5* mutant to an apparently normal wild-type size. This is consistent with our in vitro observation that none of these mutations affected general autophosphorylation of the BRI1 cytoplasmic domain; thus, phosphorylation at these residues is unlikely to serve an autoinhibitory role in vivo. However, based on our in vitro peptide assay, we expected that some of these mutations might show an altered phenotype as a result of inability to phosphorylate a downstream substrate to the extent required for normal BR signaling. Moreover, the surprising increase in catalytic efficiency of the T-872-A mutation suggests that either phosphorylation at this site has a negative regulatory effect on enzyme activity or, less likely, that the substitution of Ala at this specific residue changes the protein conformation to a more active state.

Although T1 plants are adequate for a qualitative assay of *bri1-5* rescue, it is possible that the juxtamembrane and/or C-terminal mutations have subtle phenotypes as a result of altered phosphorylation of substrates in a specific branch pathway of BR signal transduction. In fact, many of the juxtamembrane transgenic lines appeared to have altered leaf morphology and petiole length, and many of the T-872-A transgenic lines appeared larger than control plants, which is consistent with in vitro data. To test these possibilities further, we are currently generating homozygous T3 lines for each mutation that will be subjected to a detailed morphometric analysis of several growth parameters. Second, as in the TGF-β model, it is possible that one member of the heterodimer (in this case BAK1) is primarily responsible for downstream signaling and that juxtamembrane or C-terminal mutations do not affect the ability of BRI1 to activate BAK1 via phosphorylation. These mutations might still affect the phosphorylation of an in vivo BRI1 substrate that is not involved in a major aspect of BR signaling, which would reconcile the in vitro peptide assay results with the in planta data. A third explanation for the apparent difference between in vitro and in vivo results might be that multiple phosphorylation sites are required to generate a substrate docking site and that elimination of phosphorylation at a single site is not sufficient to eliminate substrate interaction in vivo. Finally, we used the *bri1-5* mutant because of its clear phenotypic differences from the wild type and because it is fertile, allowing use of the floral dip procedure of Arabidopsis transformation that is not possible with *bri1* null alleles. Transformation of severe *bri1* alleles by root explant procedures can lead to artifacts in tissue culture and regeneration that make phenotypic analysis more difficult. However, because *bri1-5* is not a null allele, it is possible that dimerization of the transgene (having a wild-type extracellular domain and a mutated kinase domain) with endogenous *bri1-5* (having a defective extracelluar domain but a wild-type kinase domain) might generate an active signaling pair. However, the activation loop mutations, which would form a dimer of similar conformation, were not able to rescue the *bri1-5* phenotype, and our previous results (Oh et al., 2000) showed that autophosphorylation of BRI1 occurs by an intramolecular mechanism, which would argue against signaling through the *bri1-5*/transgene pair.

With respect to activation loop substitutions, T-1039-A and S-1042-A had a more moderate effect on autophosphosphorylation in vitro and in planta signaling than the T-1049 and S/T-1044/5 mutants. However, BAK1 was autophosphorylated in vitro on residues equivalent to both BRI1 T-1039 and S-1042. Moreover, the AtSERK1 residue T-462, corresponding to BRI1 S-1042, was found to affect substrate phosphorylation more than autophosphorylation in vitro (Shah et al., 2001), which was also observed for BRI1 T-1039-A and S-1042-A. Thus, one or both of these BRI1 residues might be true sites of phosphorylation in vivo. The profound effect of S-1044-A and/or T-1045-A and T-1049-A substitutions on autophosphorylation, peptide substrate phosphorylation in vitro, and in planta signaling we observed here suggests that phosphorylation of at least two of these activation loop residues is essential for BRI1 kinase function. Moreover, even when expressed from the native BRI1 promoter, some S/T-1044/45 and T-1049-A lines resulted in a smaller phenotype than untransformed *bri1-5*, suggesting a dominant negative effect similar to that observed when a kinase-inactive BAK1 was overexpressed from the *Cauliflower mosaic virus* 35S promoter in *bri1-5* (Li et al., 2002). Replacement of the partially active bri1-5 protein with the completely inactive S/T-1044/45 and T-1049-A mutant kinases in BRI1/BAK1 heterodimers could lead to a further reduction in BR signaling in these transgenic lines and a resulting dwarf phenotype more severe than untransformed *bri1-5* mutants. Interestingly, two different point mutations in the activation loop of the related RLK, CLAVATA1 (CLV1), both lead to an intermediate dominant negative phenotype (Dievart et al., 2003). Although neither of these mutations occurs in the four Ser residues within the CLV1 activation loop, *clv1-1* is a G-856-D substitution immediately preceding S-857, which corresponds to

Figure 8. (continued).

each construct are shown. All lines were grown under the same conditions and are the same age (32 d). Transgene expression was monitored by immunoblot analysis with anti-Flag antibody using equal amounts of protein from each plant. Cosuppression was examined by assaying native BRI1 RNA levels using competitive RT-PCR on equal amounts of total RNA isolated from each plant. The synthetic RNA competitor had the same sequence (except for a 53-nucleotide deletion in the center of the fragment) and used the same primer pair as endogenous BRI1. Lanes marked (−) had no reverse transcriptase and verified lack of DNA contamination.

BRI1 T-1049. It would be highly informative to determine if S-857 is phosphorylated in vivo in CLV1 and if the *clv1-1* mutation affected this putative phosphorylation.

Ser or Thr residues occur in the position equivalent to BRI1 T-1049, seven amino acids N-terminal to the end of the activation loop, in >99% of Arabidopsis RD-type LRR RLKs, suggesting that this may be a critical site of in vivo phosphorylation in many of these proteins, and indeed at least four Arabidopsis RLKs are phosphorylated on this residue in vivo (Nuhse et al., 2004). We also confirmed by LC/MS/MS analysis that BAK1 was autophosphorylated in vitro on the corresponding Thr residue (T-455 in BAK1). Similarly, it was previously shown by a T-468-A substitution that the corresponding Thr in AtSERK1 was essential for both autophosphorylation and substrate phosphorylation in vitro (Shah et al., 2001). Furthermore, the *Lotus japonicus* SYMBIOSIS RECEPTOR KINASE was shown by LC/MS/MS to be autophosphorylated in vitro on the corresponding residue (T-760), and T-760-A substitutions significantly reduced kinase activity in vitro (Yoshida and Parniske, 2005). Another activation loop residue, S-754, was also phosphorylated in vitro in this RLK, which aligns with S-1044 in BRI1. S-1044 is much more conserved in RLK alignments than T-1045 (Figure 4).

Based on conservation of function in other RLKs and our own in vitro and in vivo data, we propose that BL-dependent phosphorylation of T-1049 and S-1044 are required for activation and function of BRI1 in planta. Based on biochemical analysis, phosphorylation of juxtamembrane and C-terminal Ser and Thr residues might affect further phosphorylation of BRI1 cytoplasmic substrates but apparently is not required for general kinase activation.

METHODS

Plant Growth and Protein Extraction

Arabidopsis thaliana plants were grown in shaking liquid culture as previously described (Clouse et al., 1993). For BRI1/BAK1 interaction studies and BL-dependent phosphorylation analysis, either 1 μM BRZ 22012 or 2 μM BRZ 220, or a solvent control was added after 6 d of culture to transgenic plants expressing both BRI1-Flag and BAK1-GFP (Li et al., 2002). Growth was continued an additional 5 d, and plants were treated with 0.1 μM BL or a solvent control for 1.5 h before harvest. For analysis of in vivo phosphorylation sites by LC/MS/MS, plants expressing only BRI1-Flag (Li et al., 2002) were grown for 11 d without BRZ treatment, followed by BL treatment as above. Total membrane protein was isolated by grinding 15 to 20 g of tissue in liquid N_2 followed by further grinding in 50 mL of cold 20 mM Tris-HCl, pH 8.8, 150 mM NaCl, 1 mM EDTA, 20% glycerol, 1 mM phenylmethylsulfonyl fluoride (PMSF), 20 mM NaF, 50 nM microcystin, and protease inhibitor cocktail tablets (Roche Diagnostics, Indianapolis, IN). The extract was spun at 6000*g* for 15 min (4°C), and the resultant supernatant was further centrifuged at 100,000*g* for 2 h (4°C) to precipitate the total membrane fraction. The pellet was resuspended in 1 to 2 mL of 10 mM Tris-HCl, pH 7.3, 150 mM NaCl, 1 mM EDTA, 10% glycerol, 1% Triton X-100, 1 mM PMSF, 20 mM NaF, 500 nM microcystin, and protease inhibitor cocktail (Roche) and sonicated. The sample was clarified by centrifugation, and total membrane protein in the supernatant was quantified as described (Bradford, 1976). Membrane protein was adjusted to 0.5 to 1.0 mg/mL, and Triton X-100 was reduced to 0.2% before immunoprecipitation.

Immunoprecipitation and Immunoblot Analysis

BRI1-Flag was immunoprecipitated with prewashed anti-Flag M_2 affinity gel (Sigma-Aldrich, St. Louis, Mo) at 4°C overnight, washed extensively, and eluted with 100 μL of 1.5× SDS sample loading buffer (3% SDS, 94 mM Tris-HCl, pH 6.8, 15% glycerol, and 7.5% β-mercaptoethanol). After boiling for 5 min, 5 μL of supernatant was separated by 8% PAGE. BAK1-GFP was immunoprecipitated from solubilized total membrane protein using anti-GFP mouse antibody (Molecular Probes) followed by protein A beads (Pierce, Rockford, IL). Immunoprecipitated proteins were detected by immunoblot analysis on PVDF membranes with anti-Flag M_2 antibody (Sigma-Aldrich) at 1:5000 dilution, anti-GFP antibody (Molecular Probes) at 1:2000, or antiphosphothreonine antibody (Cell Signaling Biotechnology, Beverly, MA) at 1:1000. Blots were developed with horseradish peroxidase–linked secondary antibodies and the ECL chemiluminesence detection system (Amersham Biosciences, Piscataway, NJ).

Determination of in Vivo Phosphorylation Sites by QTOF LC/MS/MS

BRI1-Flag was immunoprecipitated from BL-treated Arabidopsis plants as described above except that 50 μL of concentrated immunoprecipitate (minus β-mercaptoethanol) was separated by SDS-PAGE. Gels were stained with Sypro Ruby (Molecular Probes), and the BRI1-Flag band was excised. In-gel digestion with typsin was performed according to a published protocol (Rowley et al., 2000). After digestion, peptides were extracted and desalted using a modified vented column similar to that previously described (Yi et al., 2003). Briefly, the extracted peptides were desalted on a 100 μm × 2-cm homebuilt trapping column packed with Jupiter Proteo C18 packing material (Phenomenex, Torrance, CA). The bound peptides were then flushed onto a 10 cm × 75-μm New Objectives Picofrit column (Woburn, MA) packed with Jupiter Proteo stationary phase and eluted for 50 min with a gradient of 5% B to 50% B for 30 min (mobile phase A = 0.1% formic acid in water; mobile phase B = 0.1% formic acid in 95% acetonitrile) into a Waters Q-ToF Ultima mass spectrometer with a flow rate of 250 nL/min. The top four ions in each survey scan were then subjected to automatic low energy CID, and the resulting uninterpreted MS/MS spectra were searched against the Arabidopsis protein database using the Mascot 2.0 searching algorithm (Matrix Science, London, UK) with an in-house server.

Determination of in Vivo Phosphorylation Sites by Ion Trap LC/MS/MS

In-Gel Tryptic Digestion

BRI1-Flag immunoprecipitation from Arabidopsis plants and SDS-PAGE was as described above for QTOF LC/MS/MS. A gel slice containing ~2 μg of BRI1-Flag was destained in acetonitrile/50 mM NH_4HCO_3, pH 8.0, (1/1, v/v), dehydrated in 75% acetonitrile, and dried in a vacuum centrifuge. The gel slice was incubated at 55°C for 1 h in reducing solution (10 mM DTT and 100 mM NH_4HCO_3, pH 8.0), then alkylated in 25 mM NH_4CO_3 and 20 mM iodoacetamide at 37°C for 30 min. The gel slice was washed with 25 mM NH_4CO_3 and dehydrated as before. The slice was then crushed into smaller pieces and rehydrated with 30 μL of 50 mM NH_4HCO_3, pH 8.0, containing enough trypsin to provide a 1:5 trypsin-to-protein ratio, and then incubated overnight at 37°C. After proteolysis, the peptides were extracted three times by adding 0.2 mL of 60% acetonitrile/5% formic acid (v/v) to each sample followed by sonication for 30 min in a sonicating bath. The pooled extracts were lyophilized and stored at −80°C until LC/MS/MS analysis could be performed. The dried peptides were resuspended in 25 μL of 5% acetonitrile/0.1% formic acid, of which 8 μL was used for microcapillary reverse-phase LC/MS/MS (rp-μLC/MS/MS) analysis.

rp-μLC/MS/MS

Peptide samples were analyzed using an Agilent 1100 series capillary LC system (Agilent Technologies, Palo Alto, CA) coupled directly online with an LCQ Deca ion trap mass spectrometer (Thermo Finnigan, San Jose, CA). The instrument was equipped with an in-house manufactured electrospray interface and operated in positive ion mode with an electrospray voltage of 2.2 kV (Qian et al., 2003). The reverse-phase capillary HPLC column containing 5 μm Jupiter C_{18} stationary phase (Phenomenex) was slurry packed in house into a 150-μm i.d. × 60-cm length capillary (Polymicro Technologies, Phoenix, AZ). The mobile phase consisted of (A) 0.1% formic acid in water and (B) 0.1% formic acid in acetonitrile. After loading a sample volume of 8 μL onto the reverse-phase column, the mobile phase was held at 5% B for 20 min and the peptides were eluted using a linear gradient to 95% B for 90 min at a flow rate of 1.5 μL/min. The data acquisition sequence used for all LC/MS/MS analyses employed a full MS scan followed by four MS/MS scans, where the four most intense ions were dynamically selected from the precursor MS scan and subjected to CID using a normalized collision energy setting of 45%.

Enrichment of Phosphopeptides Using IMAC

Peptide sample remaining after the initial rp-μLC/MS/MS analysis (17 μL) was enriched for phosphopeptides using an IMAC spin column from Pierce. An equal volume of 5% acetic acid was added to the sample, which was then applied to the dehydrated column media where sample absorption was complete within 5 min at room temperature. The unretained pepides were removed by spinning the column at 3000 rpm for 1 min, followed by two washes of 50 μL of 0.1% acetic acid, two washes of 50 μL of 0.1% acetic acid/10% acetonitrile (v/v), and one wash of 75 μL of water. The enriched phosphopeptides were eluted with two 20-μL aliquots of 100 mM NH_4HCO_3, pH 8.5, which were pooled, lyophilized, and stored at −80°C. The dried peptides were resuspended in 10 μL of 0.1% formic acid/5% acetonitrile (v/v), of which 8 μL was used for rp-μLC/MS/MS analysis as above.

Peptide Identification

Peptides were identified by searching the MS/MS spectra against a database containing the BRI1-Flag protein sequence using TurboSEQUEST as provided in BioWorks 3.1 (Thermo Finnigan). All of the spectra were analyzed using a dynamic mass modification (i.e., residue masses equal to the presence or absence of the modification) on Ser, Thr, and Tyr residues corresponding to the additional mass of HPO_3 (80.0 D). In addition, all oxidation states of Met residues (16.0 D for Met sulfoxide and 32.0 D for Met sulfone) and alkylated Cys residues (57.0 D) were used as static modifications (i.e., residue masses requiring the presence of the modification) during each search. Only tryptic peptides displaying a charge dependent cross-correlation score (Xcorr) of 2.0, 1.5, and 3.3, for +1, +2, and +3 charged species, respectively, and a Δ-correlation score (ΔC_n) of at least 0.1 were used for positive identification similar to that previously reported (Peng et al., 2003). For phosphopeptides, each MS/MS spectrum was manually inspected to ensure acceptable ion coverage and phosphorylation site identification.

Determination of BAK1 in Vitro Phosphorylation Sites by Ion Trap LC/MS/MS

Purified recombinant GST-BAK1 was autophosphorylated in vitro as described (Li et al., 2002) except that only unlabeled ATP was used. Protein bands were excised from PAGE gels and in-gel digested as described for BRI1. Samples were analyzed at the Taplin Biological Mass Spectrometry Facility (Harvard University, Cambridge, MA) with an LCQ DECA ion trap mass spectrometer. Identification of phosphorylated and nonphosphorlyated peptides was performed by SEQUEST analysis as above. Sequence coverage of the BAK1 cytoplasmic domain was 56%.

Site-Directed Mutagenesis of the Flag-BRI1 Cytoplasmic Domain

The previously described Flag-BRI-KD construct (Oh et al., 2000) consisting of an 11–amino acid N-terminal Flag tag (DYKDDDDKVKL) followed by amino acids 815 through 1196 of BRI1, cloned into pFLAG-MAC (Sigma-Aldrich), was used as the template for site-directed mutagenesis with the Quick Change II site-directed mutagenesis kit (Stratagene, La Jolla, CA). Seventeen individual constructs were generated with the following substitutions: S-838-A, T-842-A, T-846-A, S-858-A, T-872-A, T-880-A, S-887-A, S-891-A, T-982-A, T-1039-A, S-1042-A, S/T-1044/5-A, T-1049-A, S-1168-A, S-1172-A, S/T-1179/80-A, and S-1187-A. All constructs were sequenced to verify specific mutations and lack of other unexpected mutations.

Recombinant Protein Purification and in Vitro Phosphorylation Assays

Overexpression of Flag-BRI1-KD and its mutations in BL21 (DE3) pLysS cells and purification on anti-FLAG M_2 affinity gels were conducted as described in the manufacturer's instructions (Sigma-Aldrich) with some modifications. Proteins were induced with 0.5 mM IPTG at 30°C for 3 h. The frozen cells pellets from 500 mL of bacterial culture were suspended in 50 mL buffer A (50 mM Tris-HCl, pH 8.0, 5 mM EDTA, pH 8.0, and 0.25 mg/mL of lysozyme) and incubated for 5 min at 25°C. Five mL of buffer B was added (1.5 M NaCl, 0.1 M $CaCl_2$, 0.1 M $MgCl_2$, 10 mM PMSF, 100 mM β-mercaptoethanol, 40 μg/mL of DNase I, and protease inhibitor cocktail tablets [Roche Diagnostics]) followed by incubation at 25°C for 5 min. Other manipulations were performed as described in the Sigma-Aldrich protocol. Kinase assays for autophosphorylation were as described previously (Li et al., 2002). A volume of each autophosphorylation reaction containing 1 μg of protein was separated by SDS-PAGE, and the gel was stained, dried, and autoradiographed. Peptide substrate phosphorylation assays were performed basically as previously described (Oh et al., 2000). Synthetic peptide BR13 (GRJKKIASVEJJKK, where J, nor-Leu, is a nonoxidizing functional equivalent of Met) was purified to >90% by reverse-phase HPLC. Each experimental point was determined in triplicate.

In Vivo Functional Analysis of BRI1-Flag Phosphorylation Sites

A complex series of PCR amplifications and subclonings into intermediate vectors gave rise to a series of 19 constructs each containing 1699 bp of the BRI1 5′ upstream genomic and untranslated regions (from ecotype Ws-2) followed by the entire BRI1 coding sequence (either wild-type, K-911-E kinase-inactive, or the 17 S/T-to-A substitutions described above for Flag-BRI1-KD). Each construct terminated with an in-frame Flag epitope tag and was contained in the pBIB-Hyg binary plant transformation vector (Becker et al., 1992; Li et al., 2002). All DNA constructs were sequence verified, and each construct was transformed individually into *bri1-5* (Ws-2 background) by the floral dipping *Agrobacterium tumefaciens*–mediated transformation method (Clough and Bent, 1998). T1 seedlings growing at 22°C were screened on MS medium with 35 μg/mL of hygromycin for 3 weeks. Putative transformants were transplanted into soil pots and placed in a growth chamber at 18 to 20°C and a 16-h-light/8-h-dark photoperiod.

To examine BRI1-Flag transgene expression in independent transgenic lines, 50 mg of young leaves from approximately the same position in the plant were ground in liquid N_2, followed by the addition of 200 μL 2% SDS (w/v), 62.5 mM Tris-HCl, pH 6.8, 5% β-mercaptoethanol, and 10% glycerol, with further grinding. The homogenate was boiled for 5 min and centrifuged for 15 min at 10,000*g*. The supernatant was collected, and

protein concentration was determined according to Bradford (Bradford, 1976). Samples containing 50 μg of protein were subjected to SDS-PAGE and electroblotted to a PVDF membrane. Immunoblot analysis was performed with Anti-Flag M_2 monoclonal antibody (Sigma-Aldrich) as described above.

To assess native BRI1 expression in the transgenic lines and to test for possible cosuppression, competitive RT-PCR was employed. Competitor preparation and RT-PCR conditions were as described in the RT-PCR competitor construction kit manual (Ambion, Austin, TX). The DNA template for competitor RNA in vitro transcription was obtained by PCR amplifying Arabidopsis Ws-2 genomic DNA with the primers 5′-GCGTAATACGACTCACTATAGGGAGAGGAGAGGAAGATCCAGCATTAGAGTTGGAGACGACCGACAATG-3′ and 5′-ACTTTCCCATTCCCGTGCAG-3′. The competitor template was identical to native BRI1, with the exception of a 53-bp deletion in the central portion of the sequence. For the competitor RNA in vitro transcription reaction, 0.3 μg of purified DNA template was used with T7 RNA polymerase in a 20-μL reaction volume at 37°C overnight. The DNA template was then digested with RNase-free DNase I, and full-length competitor RNA was separated by 4.5% PAGE. Competitor RNA was extracted from the gel and the number of copies calculated.

For total RNA isolation from transgenic plants, 50 mg of leaves were harvested as above and ground in liquid N_2. Six hundred microliters of CTAB (hexadecyltrimethylammobiumbromide) extraction buffer (100 mM Tris-HCl, pH 8.0, 1.4 M NaCl, 20 mM EDTA, and 2% CTAB) was added with further grinding. The homogenate was incubated at 60 to 65°C for 20 to 30 min and extracted with chloroform two times. RNA was precipitated with 0.3 volumes of 10 M $LiCl_2$ at −20°C overnight, followed by centrifugation for 15 min at 12000*g*. Resuspended RNA was digested with RNase-free DNase I. For RT-PCR, 5 μg of total RNA was mixed with 10^8 copies of the competitor in a 20-μL reaction volume and incubated as described with Moloney murine leukemia virus reverse transcriptase (Ambion). One microliter of the 20-μL reaction was used for the PCR reaction with primers 5′-AGGAAGATCCAGCATTAGAG-3′ and 5′-ACATACACTTAGCATATAGTAG-3′, yielding fragments of 354 and 301 bp for native BRI1 and its competitor, respectively. The second primer hybridized with sequences in the BRI1 3′ untranslated region that are not present in the transgene (which contains a nopaline synthase 3′ untranslated region); thus, RT-PCR specifically amplified native BRI1 and not BRI1-Flag.

ACKNOWLEDGMENTS

LC/MS/MS analysis of the in vitro sites of GST-BAK1 was performed by Ross Tamaino of the Taplin Biological Mass Spectrometry Facility (Harvard University, Cambridge, MA). We thank Gregory Scott (North Carolina State University, Raleigh, NC) for excellent technical assistance. This work was supported by grants from the National Science Foundation (MCB-0419819), the USDA competitive grants program (NRI 2004-35304-14930 and NRI 2001-35304-10886), and the North Carolina Agricultural Research Service. X.W. is a visiting scholar on leave from Northwestern Sci-Tech University of Agriculture and Forestry (Shaanxi, China).

Received February 2, 2005; revised April 20, 2005; accepted April 20, 2005; published May 13, 2005.

REFERENCES

Adams, J.A. (2003). Activation loop phosphorylation and catalysis in protein kinases: Is there functional evidence for the autoinhibitor model? Biochemistry **42,** 601–607.

Altmann, T. (1999). Molecular physiology of brassinosteroids revealed by the analysis of mutants. Planta **208,** 1–11.

Asami, T., Min, Y.K., Nagata, N., Yamagishi, K., Takatsuto, S., Fujioka, S., Murofushi, N., Yamaguchi, I., and Yoshida, S. (2000). Characterization of brassinazole, a triazole-type brassinosteroid biosynthesis inhibitor. Plant Physiol. **123,** 93–100.

Baxter, R.M., Secrist, J.P., Vaillancourt, R.R., and Kazlauskas, A. (1998). Full activation of the platelet-derived growth factor beta-receptor kinase involves multiple events. J. Biol. Chem. **273,** 17050–17055.

Becker, D., Kemper, E., Schell, J., and Masterson, R. (1992). New plant binary vectors with selectable markers located proximal to the left T-DNA border. Plant Mol. Biol. **20,** 1195–1197.

Becraft, P.W. (2002). Receptor kinase signaling in plant development. Annu. Rev. Cell Dev. Biol. **18,** 163–192.

Binns, K.L., Taylor, P.P., Sicheri, F., Pawson, T., and Holland, S.J. (2000). Phosphorylation of tyrosine residues in the kinase domain and juxtamembrane region regulates the biological and catalytic activities of Eph receptors. Mol. Cell. Biol. **20,** 4791–4805.

Bishop, G.J. (2003). Brassinosteroid mutants of crops. J. Plant Growth Regul. **22,** 325–335.

Bradford, M.M. (1976). A rapid and sensitive method for the quantitation of microgram quantities of protein utilizing the principle of protein-dye binding. Anal. Biochem. **72,** 248–254.

Clough, S.J., and Bent, A.F. (1998). Floral dip: A simplified method for Agrobacterium-mediated transformation of *Arabidopsis thaliana*. Plant J. **16,** 735–743.

Clouse, S.D. (2002). Brassinosteroid signal transduction. Clarifying the pathway from ligand perception to gene expression. Mol. Cell **10,** 973–982.

Clouse, S.D., Hall, A.F., Langford, M., McMorris, T.C., and Baker, M.E. (1993). Physiological and molecular effects of brassinosteroids on *Arabidopsis thaliana*. J. Plant Growth Regul. **12,** 61–66.

Clouse, S.D., Langford, M., and McMorris, T.C. (1996). A brassinosteroid-insensitive mutant in *Arabidopsis thaliana* exhibits multiple defects in growth and development. Plant Physiol. **111,** 671–678.

Clouse, S.D., and Sasse, J.M. (1998). Brassinosteroids: Essential regulators of plant growth and development. Annu. Rev. Plant Physiol. Plant Mol. Biol. **49,** 427–451.

Cock, J.M., Vanoosthuyse, V., and Gaude, T. (2002). Receptor kinase signalling in plants and animals: Distinct molecular systems with mechanistic similarities. Curr. Opin. Cell Biol. **14,** 230–236.

Dievart, A., Dalal, M., Tax, F.E., Lacey, A.D., Huttly, A., Li, J., and Clark, S.E. (2003). CLAVATA1 dominant-negative alleles reveal functional overlap between multiple receptor kinases that regulate meristem and organ development. Plant Cell **15,** 1198–1211.

Eng, J.K., McCormak, A.L., and Yates, J.R. (1994). An approach to correlate tandem mass spectral data of peptides with amino acid sequences in a protein database. J. Am. Soc. Mass Spectrom. **5,** 976–989.

Guo, L., Kozlosky, C.J., Ericsson, L.H., Daniel, T.O., Cerretti, D.P., and Johnson, R.S. (2003). Studies of ligand-induced site-specific phosphorylation of epidermal growth factor receptor. J. Am. Soc. Mass Spectrom. **14,** 1022–1031.

Guo, Y., Qiu, Q.-S., Quintero, F.J., Pardo, J.M., Ohta, M., Zhang, C., Schumaker, K.S., and Zhu, J.-K. (2004). Transgenic evaluation of activated mutant alleles of SOS2 reveals a critical requirement for its kinase activity and C-terminal regulatory domain for salt tolerance in *Arabidopsis thaliana*. Plant Cell **16,** 435–449.

Haffani, Y.Z., Silva, N.F., and Goring, D.R. (2004). Receptor kinase signalling in plants. Can. J. Bot. **82,** 1–15.

Hubbard, S.R. (2004). Juxtamembrane autoinhibition in receptor tyrosine kinases. Nat. Rev. Mol. Cell Biol. **5,** 464–471.

Huse, M., and Kuriyan, J. (2002). The conformational plasticity of protein kinases. Cell **109,** 275–282.

Huse, M., Muir, T.W., Xu, L., Chen, Y.G., Kuriyan, J., and Massague, J. (2001). The TGF beta receptor activation process: An inhibitor- to substrate-binding switch. Mol. Cell **8,** 671–682.

Johnson, L.N., Noble, M.E., and Owen, D.J. (1996). Active and inactive protein kinases: Structural basis for regulation. Cell **85,** 149–158.

Kalo, M.S., and Pasquale, E.B. (1999). Multiple *in vivo* tyrosine phosphorylation sites in EphB receptors. Biochemistry **38,** 14396–14408.

Kauschmann, A., Jessop, A., Koncz, C., Szekeres, M., Willmitzer, L., and Altmann, T. (1996). Genetic evidence for an essential role of brassinosteroids in plant development. Plant J. **9,** 701–713.

Kinoshita, T., Cano-Delgado, A., Seto, H., Hiranuma, S., Fujioka, S., Yoshida, S., and Chory, J. (2005). Binding of brassinosteroids to the extracellular domain of plant receptor kinase BRI1. Nature **433,** 167–171.

Lease, K., Ingham, E., and Walker, J. (1998). Challenges in understanding RLK function. Curr. Opin. Plant Biol. **1,** 388–392.

Li, J., and Chory, J. (1997). A putative leucine-rich repeat receptor kinase involved in brassinosteroid signal transduction. Cell **90,** 929–938.

Li, J., Wen, J., Lease, K.A., Doke, J.T., Tax, F.E., and Walker, J.C. (2002). BAK1, an Arabidopsis LRR receptor-like protein kinase, interacts with BRI1 and modulates brassinosteroid signaling. Cell **110,** 213–222.

Liu, G.Z., Pi, L.Y., Walker, J.C., Ronald, P.C., and Song, W.Y. (2002). Biochemical characterization of the kinase domain of the rice disease resistance receptor-like kinase XA21. J. Biol. Chem. **277,** 20264–20269.

Loyet, K.M., Stults, J.T., and Arnott, D. (2005). Mass spectrometric contributions to the practice of phosphorylation site mapping through 2003: A literature review. Mol. Cell Proteomics **4,** 235–245.

Massague, J. (1998). TGF-beta signal transduction. Annu. Rev. Biochem. **67,** 753–791.

Nam, K.H., and Li, J. (2002). BRI1/BAK1, a receptor kinase pair mediating brassinosteroid signaling. Cell **110,** 203–212.

Noguchi, T., Fujioka, S., Choe, S., Takatsuto, S., Yoshida, S., Yuan, H., Feldmann, K., and Tax, F. (1999). Brassinosteroid-insensitive dwarf mutants of Arabidopsis accumulate brassinosteroids. Plant Physiol. **121,** 743–752.

Nuhse, T.S., Stensballe, A., Jensen, O.N., and Peck, S.C. (2004). Phosphoproteomics of the Arabidopsis plasma membrane and a new phosphorylation site database. Plant Cell **16,** 2394–2405.

Oh, M.H., Ray, W.K., Huber, S.C., Asara, J.M., Gage, D.A., and Clouse, S.D. (2000). Recombinant brassinosteroid insensitive 1 receptor-like kinase autophosphorylates on serine and threonine residues and phosphorylates a conserved peptide motif *in vitro*. Plant Physiol. **124,** 751–766.

Pawson, T. (2002). Regulation and targets of receptor tyrosine kinases. Eur. J. Cancer **38** (suppl. 5), S3–S10.

Pawson, T. (2004). Specificity in signal transduction: From phosphotyrosine-SH2 domain interactions to complex cellular systems. Cell **116,** 191–203.

Peng, J., Elias, J.E., Thoreen, C.C., Licklider, L.J., and Gygi, S.P. (2003). Evaluation of multidimensional chromatography coupled with tandem mass spectrometry (LC/LC-MS/MS) for large-scale protein analysis: The yeast proteome. J. Proteome Res. **2,** 43–50.

Peng, P., and Li, J. (2003). Brassinosteroid signal transduction: A mix of conservation and novelty. J. Plant Growth Regul. **22,** 298–312.

Perkins, D.N., Pappin, D.J., Creasy, D.M., and Cottrell, J.S. (1999). Probability-based protein identification by searching sequence databases using mass spectrometry data. Electrophoresis **20,** 3551–3567.

Qian, W.J., Goshe, M.B., Camp II, D.G., Yu, L.R., Tang, K., and Smith, R.D. (2003). Phosphoprotein isotope-coded solid-phase tag approach for enrichment and quantitative analysis of phosphopeptides from complex mixtures. Anal. Chem. **75,** 5441–5450.

Rowley, A., Choudhary, J.S., Marzioch, M., Ward, M.A., Weir, M., Solari, R.C., and Blackstock, W.P. (2000). Applications of protein mass spectrometry in cell biology. Methods **20,** 383–397.

Russinova, E., Borst, J.W., Kwaaitaal, M., Cano-Delgado, A., Yin, Y., Chory, J., and de Vries, S.C. (2004). Heterodimerization and endocytosis of Arabidopsis brassinosteroid receptors BRI1 and AtSERK3 (BAK1). Plant Cell **16,** 3216–3229.

Schlessinger, J. (2000). Cell signaling by receptor tyrosine kinases. Cell **103,** 211–225.

Schlessinger, J. (2002). Ligand-induced, receptor-mediated dimerization and activation of EGF receptor. Cell **110,** 669–672.

Schulze-Muth, P., Irmler, S., Schroder, G., and Schroder, J. (1996). Novel type of receptor-like protein kinase from a higher plant (*Catharanthus roseus*). J. Biol. Chem. **271,** 26684–26689.

Sessa, G., D'Ascenzo, M., and Martin, G.B. (2000). Thr38 and Ser198 are Pto autophosphorylation sites required for the AvrPto-Pto-mediated hypersensitive response. EMBO J. **19,** 2257–2269.

Shah, K., Vervoort, J., and de Vries, S.C. (2001). Role of threonines in the *Arabidopsis thaliana* somatic embryogenesis receptor kinase 1 activation loop in phosphorylation. J. Biol. Chem. **276,** 41263–41269.

Shiu, S.H., and Bleecker, A.B. (2001). Receptor-like kinases from Arabidopsis form a monophyletic gene family related to animal receptor kinases. Proc. Natl. Acad. Sci. USA **98,** 10763–10768.

Thummel, C.S., and Chory, J. (2002). Steroid signaling in plants and insects—Common themes, different pathways. Genes Dev. **16,** 3113–3129.

Torii, K.U. (2004). Leucine-rich repeat receptor kinases in plants: Structure, function, and signal transduction pathways. Int. Rev. Cytol. **234**, 1–46.

Wang, B., Balba, Y., and Knutson, V.P. (1996). Insulin-induced *in situ* phosphorylation of the insulin receptor located in the plasma membrane versus endosomes. Biochem. Biophys. Res. Commun. **227,** 27–34.

Wang, Z.Y., and He, J.X. (2004). Brassinosteroid signal transduction—Choices of signals and receptors. Trends Plant Sci. **9,** 91–96.

Wang, Z.Y., Seto, H., Fujioka, S., Yoshida, S., and Chory, J. (2001). BRI1 is a critical component of a plasma-membrane receptor for plant steroids. Nature **410,** 380–383.

Yi, E.C., Lee, H., Aebersold, R., and Goodlett, D.R. (2003). A microcapillary trap cartridge-microcapillary high-performance liquid chromatography electrospray ionization emitter device capable of peptide tandem mass spectrometry at the attomole level on an ion trap mass spectrometer with automated routine operation. Rapid Commun. Mass Spectrom. **17,** 2093–2098.

Yoshida, S., and Parniske, M. (2005). Regulation of plant symbiosis receptor kinase through serine and threonine phosphorylation. J. Biol. Chem. **280,** 9203–9209.

Yu, X., Sharma, K.D., Takahashi, T., Iwamoto, R., and Mekada, E. (2002). Ligand-independent dimer formation of epidermal growth factor receptor (EGFR) is a step separable from ligand-induced EGFR signaling. Mol. Biol. Cell **13,** 2547–2557.